DETECTION OF OXIDATION IN HUMAN SERUM LIPOPROTEINS

A Thesis

by

CHRISTINE LEE MYERS

Submitted to the Office of Graduate Studies of
Texas A&M University
in partial fulfillment of the requirements for the degree of

MASTER OF SCIENCE

May 2004

Major Subject: Chemistry

DETECTION OF OXIDATION IN HUMAN SERUM LIPOPROTEINS

A Thesis

by

CHRISTINE LEE MYERS

Submitted to Texas A&M University
in partial fulfillment of the requirements
for the degree of

MASTER OF SCIENCE

Approved as to style and content by:

Ronald D. Macfarlane (Chair of Committee)	Victoria J. DeRose (Member)
Marvin W. Rowe (Member)	Rosemary L. Walzem (Member)

Emile A. Schweikert
(Head of Department)

May 2004

Major Subject: Chemistry

ABSTRACT

Detection of Oxidation in Human Serum Lipoproteins.

(May 2004)

Christine Lee Myers, B.A., The Colorado College

Chair of Advisory Committee: Dr. Ronald D. Macfarlane

A method for the oxidation of lipoproteins *in vitro* was developed using the free radical initiator, 2,2'-azobis-(2-amidinopropane) dihydrochloride (AAPH). Following *in vitro* oxidation, the susceptibility to oxidation of the serum samples was studied using density gradient ultracentifugation and matrix-assisted laser desorption/ionization time-of-flight mass spectrometry (MALDI-TOF-MS).

Shifts in mean buoyant density of the lipoprotein particles, specifically low density lipoprotein (LDL) and high density lipoprotein (HDL), were observed in the density profile following centrifugation. The degree of shift in the density proved to be proportional to the extent of oxidation. Changes in apolipoproteins were studied with MALDI-TOF-MS. Observed variations in the mass spectra include m/z shifts due to chemical modifications and change in isoform distributions.

The oxidation procedure and analysis techniques were applied to a clinical application to study the effects of table grape consumption on lipoprotein susceptibility to oxidation. The main objective of the research, to show feasibility that these methods could be used in a clinical setting, was achieved.

DEDICATION

To my family, whose continued love and support made all of this possible.

ACKNOWLEDGMENTS

I would like to express my deepest thanks to everyone who has made this research possible. I would like to thank Dr. Macfarlane, who never gave up on me. A special thanks to all my coworkers, including Dr. Brian D. Hosken, Dr. Zachlyn N. Farwig, I. Leticia Espinosa, and Richa Chandra, for their guidance, support, and friendship. I would also like to acknowledge Dr. David H. Russell and the Laboratory for Biological Mass Spectrometry, and most specifically Jody May, for acquisition of the MALDI-TOF mass spectra. Thanks to the California Table Grape Commission for generously providing the freeze-dried grape powder. Also, thanks to the College Station Scott and White laboratory for performing the blood draws. This work was supported by the NIH Heart & Lung Institute (HL 68794).

LIST OF ABBREVIATIONS

AAPH	2,2'-azobis-(2-amidinopropane) dihydrochloride
ACN	acetonitrile
Apo	apolipoproteins
BHT	butylated hydroxytoluene
CD	cardiovascular disease
CETP	cholesteryl ester transfer protein
CsBiY	cesium-bismuth-EDTA
Da	dalton
DMSO	dimethyl sulfoxide
EDTA	ethylenediaminetetracetic acid
HDL	high density lipoprotein
IDL	intermediate density lipoprotein
LCAT	lecithin:cholesterol acyltransferase
LPL	lipoprotein lipase
LDL	low density lipoprotein
M	molar
MALDI	matrix-assisted laser desorption/ionization
MDA	malondialdehyde
MCP-1	monocyte chemotactic protein-1
M-CSF	macrophage colony stimulating factor

mmLDL	minimally modified LDL
mM	milli molar
MS	mass spectrometry
MW	molecular weight
MW_{calc}	molecular weight calculated from amino acid sequence
NaBiY	sodium-bismuth-EDTA
NBD	7-nitrobenz-2-oxa-1,3-diazol-4-yl ceramide
NR	Nile Red
oxLDL	oxidized LDL
PB	phosphate buffer
PON	paraoxonase
PUFA	polyunsaturated fatty acid
SAA	serum amyloid A
TBA	thiobarbituric acid
TBARS	thiobarbituric acid reactive substances
TFA	trifluoroacetic acid
TOF	time-of-flight
UC	ultracentrifuge
UV	ultraviolet
UV/Vis	ultraviolet/visible
VLDL	very low density lipoprotein

TABLE OF CONTENTS

Page

Page

LIST OF FIGURES

FIGURE Page

FIGURE Page

LIST OF TABLES

INTRODUCTION

Complications from cardiovascular disease (CD) are the most common causes of death in western society. In their most recent report, The American Heart Association listed cardiovascular disease as the number one killer of Americans in the year 2001 (1). It has been well established that hypercholesterolemia is an important cause of CD. No matter how successfully hypercholesterolemia is dealt with, however, CD will not disappear because high cholesterol levels are by no means the only causative factors. It has become socially necessary to elucidate the mechanism of atherogenesis and find ways of dealing with the resulting diseases (2). The list of factors inducing CD is too long to thoroughly cover here.

Oxidation of lipoproteins, specifically low density lipoprotein (LDL), was discovered in the early 1980s (3). Since then, the number of papers published on oxidized LDL (oxLDL) alone has increased exponentially. Results indicate that production and accumulation of oxLDL increase in patients with vascular disease, and that oxLDL levels could provide useful diagnostic information.

Lipoproteins

Lipoproteins are complex particles in circulation that are responsible for lipid

---

This thesis follows the style and format of *Journal of Lipid Research.*

transport. Each lipoprotein particle contains a hydrophobic core of cholesterol esters and triglycerides, surrounded by a hydrophilic surface of unesterified cholesterol, phospholipids, and proteins. Also incorporated into the particle are lipid soluble antioxidant molecules such as α-tocopherol (vitamin E) and β-carotene.

Three major classes of lipoproteins exist in a human serum sample; very low density lipoprotein (VLDL), low density lipoprotein (LDL), and high density lipoprotein (HDL). There also exist other classes such as chylomicrons and intermediate density lipoprotein (IDL), as well as subclasses. These lipoprotein classes differ in their metabolic pathways, size, lipid and protein composition, and density. Table 1 summarizes the compositional differences between lipoprotein classes. Each lipoprotein, regardless of class, has a similar spherical structure.

Table 1. Composition of human serum lipoproteins (4).

Weight % of Total Lipoproteins					
Component	Chylomicrons	VLDL	IDL	LDL	HDL
Phospholipid	6-9	16-20	20-24	24-30	24-30
Free Cholesterol	1-3	4-8	8-9	9-12	2-5
Cholesteryl Esters	3-6	9-13	13-28	28-30	10-20
Triglycerides	82-86	50-60	12-50	7-11	4-5
Proteins	1-2	8-11	11-20	20-22	41-58
Density (kg/L)	0.93-1.006	0.95-1.006	1.006-1.019	1.019-1.063	1.063-1.21

While all lipoproteins are susceptible to lipid peroxidation, LDL is the most sensitive due to its composition of lipids, proteins, and antioxidant particles (5). LDL is the main cholesterol carrier in plasma. Its purpose is the transportation of cholesterol to peripheral tissues in the body. LDL is comprised of cholesterol esters and phospholipids, with very few triglycerides or unesterified cholesterol molecules. Each LDL particle contains one molecule of apolipoprotein B-100 (apo B) that acts as the receptor for LDL binding. The molecule of apo B covers much of the lipoprotein surface as shown in Figure 1, not just a small portion as often depicted in schematic sketches. The apo B alone accounts for approximately 20% of the total LDL volume (6), and acts as the ligand for the receptor that allows cholesterol influx (3). Also present are small amounts of apolipoproteins C-III and E. LDL particles exist with a variety of chemical compositions, sizes, and densities.

Evidence indicates that certain characteristics make LDL particles more or less susceptible to oxidation *in vitro*. Fatty acid composition of the lipoprotein particle is important. As polyunsaturated fatty acids (PUFAs), such as linoleic acid (18:2), are the primary source of the radical chain reaction initiation, a high proportion of PUFAs indicate greater risk of oxidation. Conversely, a high proportion of monounsaturated fatty acids, such as oleic acid (18:1) tends to protect against oxidation (7). Small dense LDL particles, which have been in circulation a longer time period than large buoyant particles, are more sensitive to *in vitro* oxidation than larger particles (8,9,10). These small particles show lower concentrations of lipid soluble antioxidants, and it has been shown *in vivo* that longer plasma residence time increases the net oxidative insult on

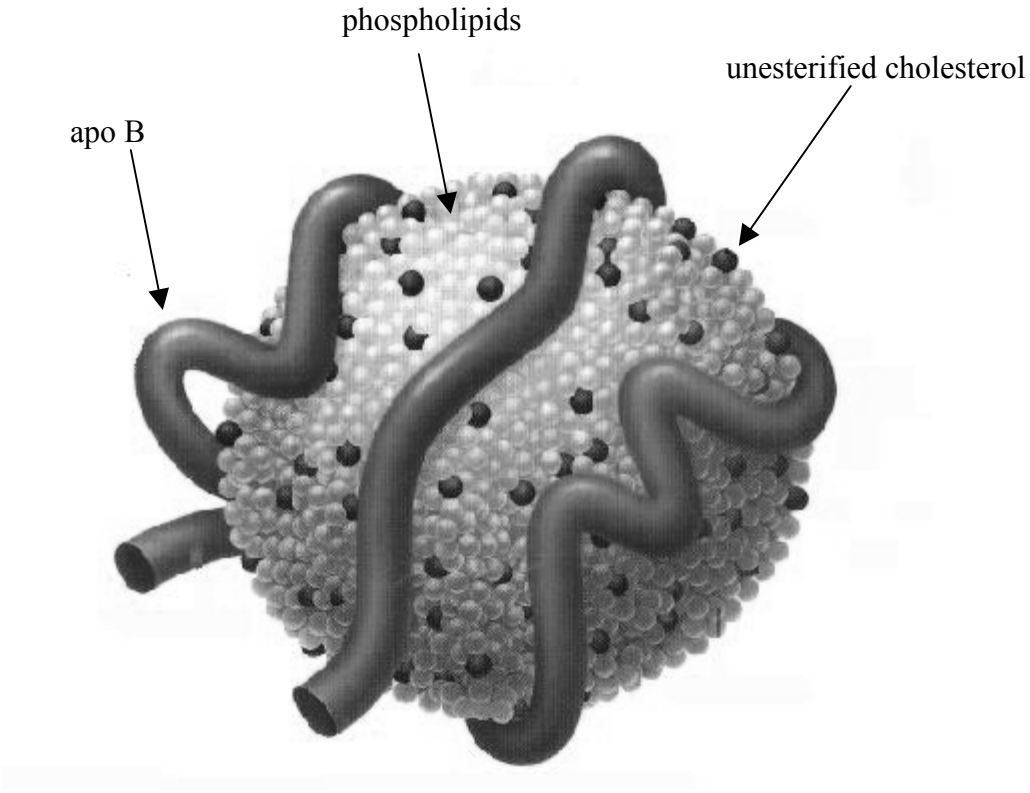

Figure 1. Structure of a low density lipoprotein (Adapted from 11).

the particle, yielding them more susceptible to oxidation (10). Increased lipoprotein glycation has also been shown to increase oxidation susceptibility due to modifications of the lipoprotein and inactivation of potential antioxidants (12). Native lipoprotein concentration, however, is not a crucial factor in the susceptibility to *in vivo* oxidation (2).

Elevated levels of LDL in serum is a predictor for CD due to LDLs ability to accumulate in the cells of the arterial intima; however native LDL is unable to initiate

foam cell formation which leads to arterial plaque. Postsecretory modifications of LDL must somehow affect its atherogenic potential.

Native LDL is taken out of the bloodstream via a receptor that recognizes a specific group of positively charged lysine residues on the apo B molecule (13). This receptor is highly regulated by cholesterol content in the peripheral tissues. An early step in atherosclerosis is the formation of a fatty streak consisting of foam cells, which are macrophages or endothelial cells laden with cholesterol. Due to its regulation, the classical LDL receptor is unable to provide a pathway for the necessary amount of cholesterol to enter the macrophages or endothelial cells for foam cell formation. This indicates there exists another receptor for LDL, known as a scavenger receptor. Patients who completely lack classical LDL receptors are still able to form foam cells, also indicating a scavenger pathway (3).

Experimentation showed that acetylation of LDL produced a modified particle that was recognized by the scavenger receptor on macrophages (14,15). No physiological evidence could support the acetylation of LDL *in vivo*, however. Similar uptake was achieved with malondialdeyhde-conjugated LDL (16), but again physiological evidence was lacking. Lipoproteins incubated with endothelial cells (17) and oxidized lipoproteins (17) are also taken up the scavenger receptor. All of these modifications increase the net negative charge of the LDL by derivatizing amino groups on the apo B molecule. For example, lysine residues, which are positively charged at physiological pH, are neutralized, thus increasing the net negative charge of the particle. Unlike some of the other modifications, oxidation could be explained by multiple

physiological mechanisms, and oxLDL has been accepted as the natural ligand for the scavenger receptor. The rate of uptake of modified particles by the scavenger receptor is much higher than uptake of native LDL by the classical receptor, and the scavenger receptor does not recognize native LDL (15,17).

In Vivo Oxidation

Oxidation of LDL affects much more than the affinity for the scavenger receptor as opposed to the classical LDL receptor. Most importantly, the lipid portion of oxLDL is cytotoxic to most cells (18,19). Oxidized particles also affect macrophage lipid loading (20), platelet aggregation, monocyte migration, can inhibit endothelial cell-dependent arterial relaxation (7), and activate the immune system (21).

The mechanism for *in vivo* oxidation of lipoproteins is believed to be a free radical driven lipid peroxidation chain reaction, shown in Figure 2. Oxidation is initiated by a free radical attack on a double bond associated with a polyunsaturated fatty acid (PUFA) in the lipoprotein. Hydrogen abstraction from the methylene (CH_2) group forms a lipid radical that quickly undergoes molecular rearrangement to a more stable form, known as a conjugated diene. The conjugated diene then reacts with molecular oxygen creating a PUFA peroxyl radical. This radical may attack an adjacent PUFA and abstract a hydrogen to form a hydroperoxide radical and yet another lipid radical. This reaction results in chain propagation. Peroxidation of other lipids also occurs, such as oxidation of cholesterol to yield oxysterols (22), and phosphatidyl choline to form lysophosphatidyl choline (23).

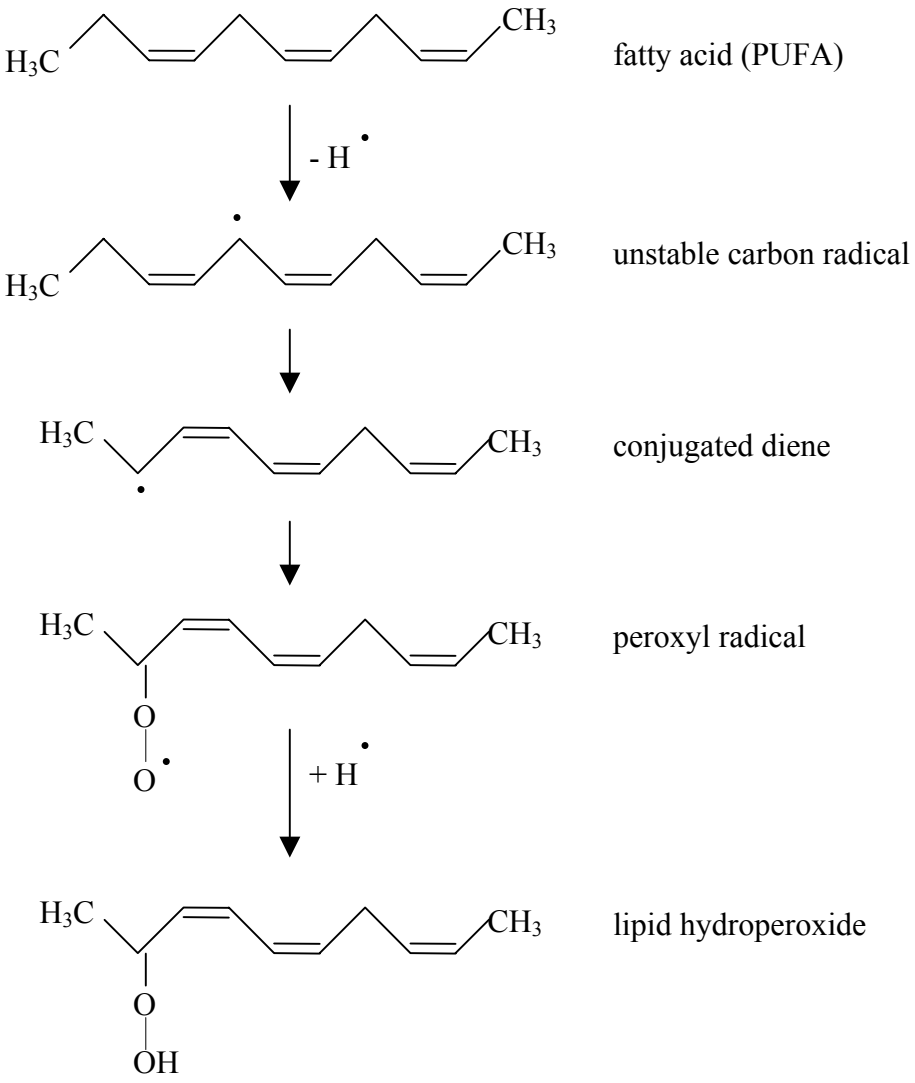

Figure 2. The chain reaction of lipid peroxidation (Adapted from 7).

Lipid hydroperoxides eventually break down into shorter chain aldehydes. These short chain aldehydes are responsible for binding to the protein constituents in the lipoprotein particles. The aldehydes bind to amino acid side chains, increasing the net

negative charge of apo B in reactions such as imination (Schiff base formation). This change in charge state makes it impossible for the oxidized LDL to bind to the classical LDL receptor. Apo B is also fragmented after exposure to lipid peroxidation byproducts.

Present in native LDL are certain antioxidants. The most predominant is the lipid soluble antioxidant α-tocopherol (vitamin E). Alpha-tocopherol scavenges peroxyl radicals and breaks the peroxidation chain reaction (24). Beta-carotene, a carotenoid and the precurser to vitamin A, is another antioxidant present in the lipoprotein. Beta-carotene quenches singlet oxygen (25). These antioxidants form radicals with such low reactivity that termination almost always occurs. Other antioxidants that are important to lipoprotein oxidation are ubiquinol (26) and HDL (27,28). HDL can itself be oxidized, however it also acts as a strong antioxidant for LDL particles. HDL contains several enzymes, such as paraoxonase (PON), that are able to cleave oxidized lipids, and therefore inhibit LDL oxidation. Apolipoprotein A-I, the major HDL lipoprotein, can remove oxidized lipids from cells, as well as influence the cell's ability to oxidize LDL particles (29).

Oxidation of lipoproteins does not occur in the anti-oxidative atmosphere of the bloodstream (30), and in fact very little fully oxidized lipoprotein circulates in the bloodstream (31). Rather, as shown in Figure 3, oxidation takes place in the extracellular space of the arterial intima (32). Native LDL particles are able to transfer in and out of the arterial wall (33). Once inside the intima, lipoproteins have less antioxidant protection and are exposed to pro-oxidants such as endothelial cells. Minimally modified LDL

(mmLDL) is formed, which is a slightly oxidized LDL particle. In mmLDL PUFA oxidation on phospholipids has occurred, but the particle is still recognizable to the classical LDL receptor (34,35). The mmLDL particles stimulate endothelial cells to release monocyte chemotactic protein-1 (MCP-1) and macrophage colony stimulating factor (M-CSF) (36). MCP-1 aids in the migration of monocytes through the endothelial membrane from the lumen to the arterial intima. Once in the subendothelial space, M-CSF induces monocyte differentiation to form macrophages. Minimally modified LDL is oxidized further until all antioxidants are depleted and the apo B is derivitized. This fully oxidized LDL particle (oxLDL) is no longer recognizable to the classical LDL receptor, but is recognized by scavenger receptors on macrophages. Uptake of oxLDL by the scavenger receptor is not regulated by intracellular cholesterol levels. Appreciable accumulation of neutral lipids therefore occurs, and the macrophage becomes laden with massive amounts of lipids. So much lipid is present that it forms lipid droplets, which characterize foam cells. Foam cells are accepted as a hallmark of early atherosclerotic lesions (2).

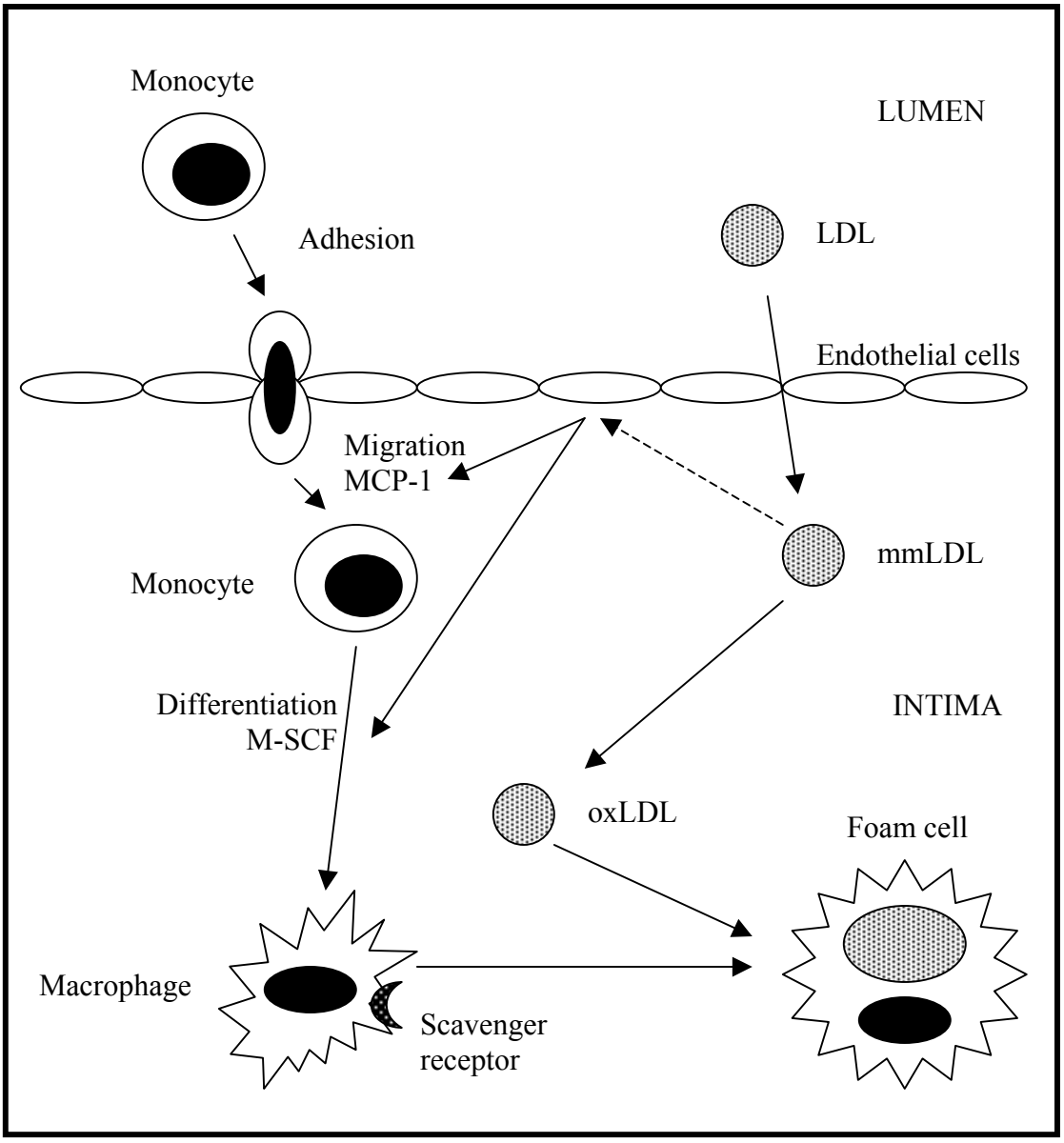

Figure 3. The role of oxLDL in atherosclerosis (36).

In Vitro Oxidation

In order to understand the *in vivo* mechanisms and consequences of oxidation, many studies have been performed *in vitro*. There are two approaches to studying oxidation *in vitro*, direct and indirect measurements. Direct measurements analyze oxidized lipoproteins or oxidation byproducts present in a plasma or serum sample. There is little oxidized lipoprotein in any plasma or serum sample as they are quickly filtered out of the bloodstream (2,31). Lack of sensitivity of the current methods for very low concentrations of oxLDL make direct measurements difficult. Some of the oxidation byproducts that can be analyzed include mmLDL, which exists in the bloodstream at higher concentrations than oxLDL, individual antioxidant concentrations, volatile hydrocarbons, and levels of auto-antibodies to oxLDL (24).

Indirect measurements take into account the susceptibility of a sample to oxidation. By exposing a sample to oxidative stress and mimicking *in vivo* oxidation, the oxidative response and therefore susceptibility to oxidation of the sample can be monitored. There are two main phases in LDL oxidation (Figure 4). The first phase, the lag phase, occurs when the lipoprotein is exposed to oxidative stress, but endogenous antioxidants protect the lipids from peroxidation. There is some oxidation of the lipids in the lipoprotein, but at a slow rate due to the protective abilities of the antioxidants. Once all the antioxidants are depleted, oxidation enters the propagation, or second, phase. The rate of oxidation increases dramatically as there is nothing left to protect the lipoprotein particle. By measuring the length of the lag phase, it is possible to determine the susceptibility of the sample and surrounding medium to oxidation.

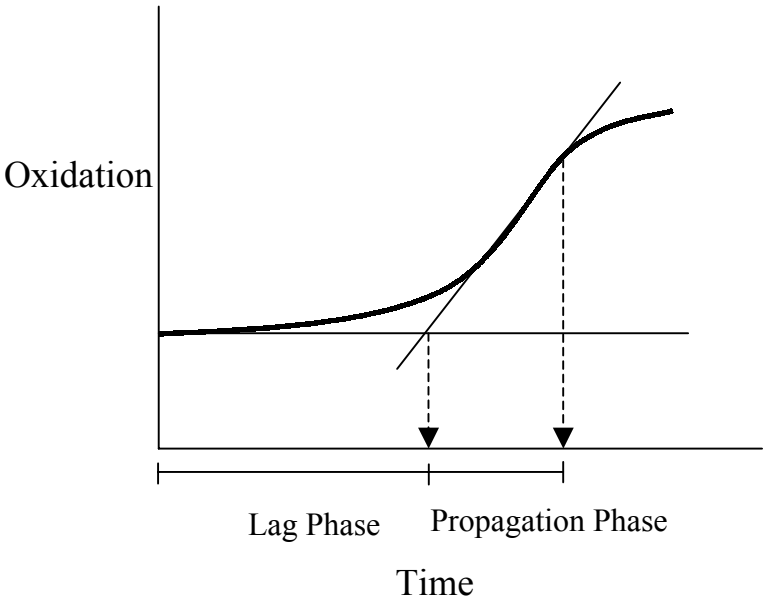

Figure 4. Typical graph of LDL oxidation.

Many physiochemical changes occur in the lipoprotein during oxidation. These multiple attributes make many types of analysis possible on intact oxidized lipoproteins, as well as byproducts from the oxidation process. Some of these attributes are listed in Table 2.

Through many *in vitro* studies, differences in lipid composition between native and oxidized LDL have been established. Following *in vitro* oxidation of LDL, there exist lower concentrations of cholesterol ester, unesterified cholesterol, phospholipids, and triglycerides (37,38) and complete consumption of endogenous antioxidants (6). Phospholipids are immobilized, showing less movement in the particle (39). Over 50%

of the phosphatidylcholine is converted to lysophosphatidylcholine (17,37,40). The increase of lysophosphatidylcholine can alter molecular ordering on the surface of the lipoprotein particle, and oxidation of core lipids can change stability and structure. Levels of conjugated dienes increase in the oxidized particle because of its stability. Aldehyde concentration in the oxidized sample also increases, as they are a final endproduct of lipid peroxidation.

Table 2. Differences in oxLDL compared to native LDL.

- Increased density
- Increased conjugated diene content
- Increased aldehyde content
- Increased electrophoretic mobility
- Decreased recognition by the classical LDL receptor
- Increased protein fragments from apo B
- Increased native fluorescence at 430 nm with excitation at 360 nm
- Decreased endogenous antioxidants

This change in lipid content is enough to affect many physiochemical properties. The buoyant density of the lipoprotein is increased significantly due to the change in lipid content, with oxLDL having densities up to 1.08 kg/L (17,40). Furthermore, examination of changes in particle density profiles can prove that the entire population of particles, not just a subpopulation, is being oxidized (41). Conjugated diene content, an intermediate in the radial chain reaction, can be easily monitored spectrophotometrically at 234 nm. Aldehyde content, too, can be used as an analysis tool. Malondialdehyde (MDA), one of the short aldehydes formed, is the peroxidation

byproduct measured in the thiobarbituric acid reactive substances (TBARS) assay. MDA is not lipid soluble, and is released from the oxidized particle into the surrounding aqueous phase (5). It is also one of the most abundant aldehydes in an oxidized sample. Another highly studied aldehyde is 4-hydroxynonenal (42).

Protein changes due to oxidation have also been elucidated using *in vitro* oxidation. It is well known that many byproducts of lipid peroxidation, especially aldehydes, have enough chemical reactivity to derivatize the apo B molecule (6,43). Apo B can also be directly modified by oxidative damage (44). In a fully oxidized LDL particle, the apo B is fragmented into shorter peptide chains, and these chains are bound to fragments of oxidized fatty acid. Most protein fragments (80-90%) remain associated with the lipoprotein particle (37).

Like lipid content, there are significant changes in amino acid content of the LDL particle before and after *in vitro* oxidation. Following oxidation, there is a decrease in reactive amino groups on the apo B molecule (37). There are significant modifications in proline, methionine, histidine, and lysine (45), which is consistent with other studies regarding the susceptibility of amino acids to oxidation (46). A significant increase in aspartic acid was also seen (45), which is compatible with previously seen oxidative opening of the histidine-imidazole ring to convert it to aspartic acid (47).

In vitro oxidation induces reactions between lipid and protein moieties. Free aldehydes react with free amino groups on lysine residues, and neutralize a cluster of positive charges (37,48). The increased negative charge on the particle results in decreased recognition by the classical LDL receptor (37,48) and increased recognition

by the scavenger receptor (49). Modification of as little as 5% of the lysine residues can result in decreased recognition by the classical LDL receptor (37). The change of charge state also results in higher electrophoretic mobility (17,50).

Some of the lipid-protein adducts that form during oxidation are N-substituted amines, or Schiff bases. These compounds contain an imine in conjunction with an electron-donating goup, often a double bond. They result in native fluorescence of the oxidized particle at 430 nm, with an excitation of 360 nm, which is characteristic of Schiff base fluorescence (5,48,51,52).

There are many ways to simulate *in vivo* oxidation. One method is by addition of azo compounds, or diazenes, which act as free radical initiators (Figure 5) (27,53,54).

$$R\text{-}N{=}N\text{-}R \rightarrow N_2 + 2R\bullet \qquad \text{(Reaction 1)}$$

$$R\bullet + R\bullet \rightarrow R\text{-}R \qquad \text{(Reaction 2)}$$

$$R\bullet + O_2 \rightarrow RO_2\bullet \qquad \text{(Reaction 3)}$$

Figure 5. Thermal decomposition of azo compounds.

Thermal decomposition of the compounds yield molecular nitrogen and two carbon radicals (Reaction 1). Because the carbon radicals are formed in close proximity, many recombine to form nonradical products (Reaction 2). Others will react with

molecular oxygen to form peroxyl radicals (Reaction 3). A specific azo compound used frequently in the oxidation of lipoproteins is 2,2'-azobis-(2-amidinopropane) dihydrochloride (AAPH) (Figure 6) (55,56,57).

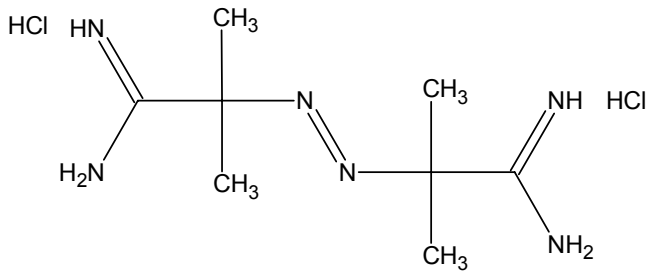

Figure 6. Structure of AAPH.

AAPH is hydrophilic, and initiates radical production in the aqueous phase. Kinetic studies have shown that the rate of decomposition is dependent on temperature, solvent, and pH. The concentration of AAPH is also important, and has been shown to be directly proportional to the radical production. In water at a pH of 7 and a temperature of 37° C, the half-life of AAPH is 175 hours. The rate of radical production can therefore be considered constant for the first few hours of any experiment (55).

AAPH has been shown to react with micelle-like particles, phospholipid liposomes, and erythrocyte membranes. It is capable of oxidizing both lipid and protein moieties (55). Structurally, lipoproteins are very similar to these particles and

comparisons of the affectivity of AAPH can be made. The precise mechanism of how AAPH and many other oxidizing agents interact with LDL remains unclear.

AAPH is not present naturally in biological systems, but it is a useful tool in studying free radical damage and inhibition nonetheless. It produces peroxyl radicals in the aqueous phase at a constant rate, which can be controlled through environmental factors. These radicals initiate the radical chain reaction that leads to complete oxidation of a lipoprotein particle. AAPH is inexpensive, and can be handled easily and safely.

Thiobarbituric Acid Reactive Substances (TBARS) Assay

The TBARS assay was first introduced in 1944 (58), and is now one of the oldest and most frequently used methods for monitoring peroxidation of biological samples. The concentration of MDA, one of the short aldehydes produced by lipid peroxidation, in a sample is believed to be proportional to the amount of oxidation. In the TBARS assay, MDA reacts with thiobarbituric acid (TBA) in an acidic environment to produce a red pigment. The pigment can then be analyzed using ultraviolet spectrophotometery at 534 nm, or fluorescence with an excitation wavelength of 515 nm.

Each MDA molecule reacts with two TBA molecules (Figure 7). The reaction is believed to be initiated by a nucleophilic attack, followed by a dehydration. This forms the 1:1 (MDA:TBA) intermediate, which then undergoes similar reactions to form the final 1:2 (MDA:TBA) adduct (59).

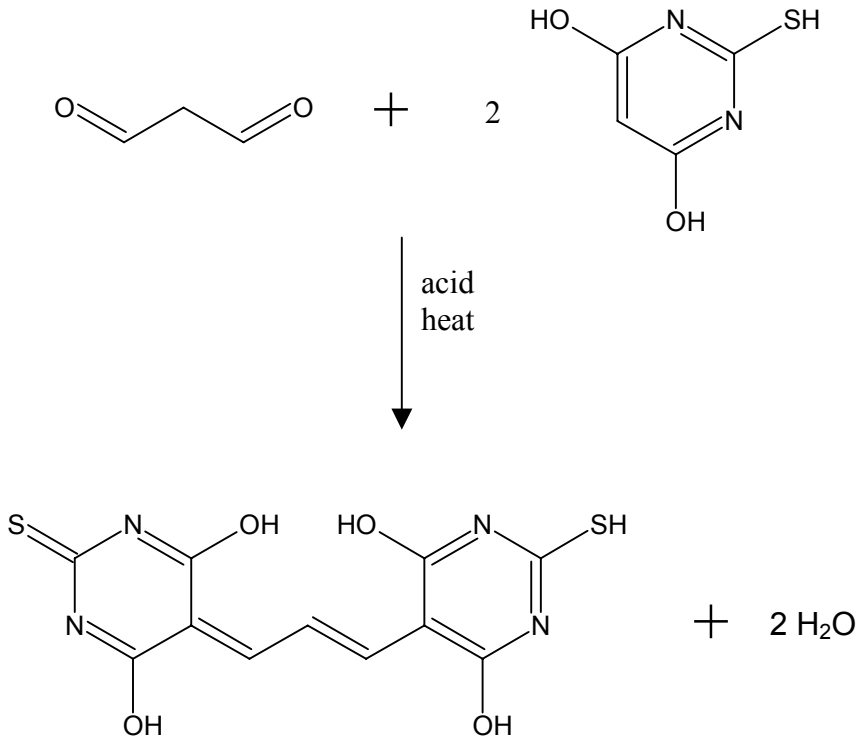

Figure 7. Formation of the TBARS pigment.

Unfortunately, the TBARS assay is not specific to MDA. The acidity and elevated temperature of the assay render most carbonyl compounds susceptible to nucleophilic attack by TBA (60). While some of the reactions yield yellow or orange chromophors that can be differentiated from the desired product, others yield red pigments that are indistinguishable from the 1:2 (MDA:TBA) adduct. Another problem with the TBARS assay is the effect of environmental variability. Many factors such as pH, type of acid used, temperature, buffers, and detergents (to list a few) can drastically alter the outcome of the assay (60).

There are two ways to calculate the concentration of MDA present in a sample; the published extinction coefficient or a calibration curve. The extinction coefficient of the MDA:TBA complex was experimentally determined to be 1.56 X 10^5 $M^{-1}cm^{-1}$ at pH 0.9 (61). Many studies still use this value while calculating total TBARS concentration, regardless of whether or not the same experimental procedure was used (62,63,64).

A calibration curve for the concentration of MDA in a sample can be produced using 1,1,3,3-tetramethoxypropane or 1,1,3,3-tetraethoxypropane (61). When placed in aqueous acid, the molecule is hydrolyzed yielding its conjugate aldehyde, MDA, and an alcohol (Figure 8).

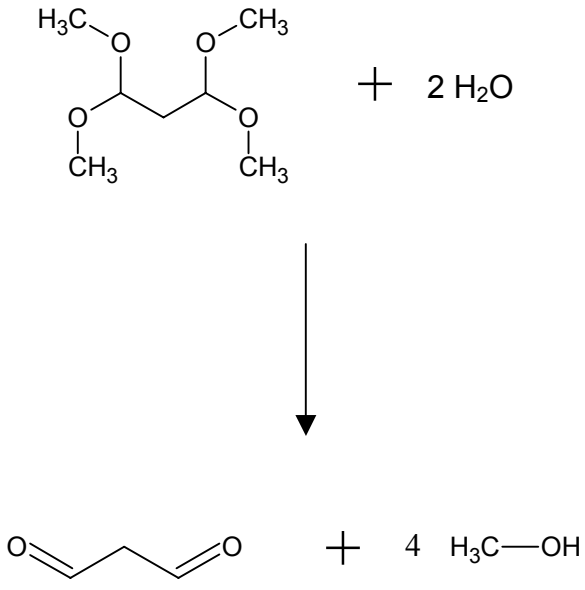

Figure 8. Hydrolysis of 1,1,3,3-tetramethoxypropane.

Reliance on a calibration curve is tenuous at best, because reaction conditions may be different between the sample and the standard to a degree that color formation is affected (60,64).

Despite a plethora of problems, the TBARS assay is still widely used. The success of the assay is due, in part, to the ease with which it can be performed. The reagents are inexpensive and easy to purchase, and most laboratories have the instrumentation necessary for analysis. While a TBARS assay is generally not the sole component of any experiment today, it is oftentimes used in conjunction with another type of analysis such as chromatography (64,65), electrophoresis (50), fluorescence detection (12,51), other assays (63, 66,67), or electron spin resonance (39).

Density Separations

Lipoproteins have historically been defined by their buoyant densities. In order to separate the lipoprotein classes used as references, ultracentrifugation was used. The methods used, however, were time consuming and tedious. More current research has developed separation methods that do not have many of the drawbacks seen previously.

Density gradient ultracentrifugation methods can be described as either rate or isopycnic separations. For rate separations, a heterogeneous environment of a sample layered either over or under a different density solution is utilized. The particles float or sediment through the density gradient at different velocities depending mainly on their buoyant densities. In isopycnic separations, the particles to be separated must be in equilibrium with the surrounding density gradient. At this point, the density of the

particles can be determined by their position in the gradient. Many separations are a mixture of the two methods. At first a separation can be based on rate as the particles move in the gradient, but as they reach equilibrium with the gradient the process becomes isopycnic.

Density gradients can be artificially created before the ultracentrifugation step, or can be self-generating during the ultracentrifugation. Self-generating gradients are easy to produce and have predictable thermodynamic properties, such as slope, concentration range, isoconcentration point, and time necessary to reach equilibrium (68). However, most require long ultracentrifugation times for gradient formation. To overcome this problem, preformed discontinuous gradients are utilized. Solutions of decreasing density are layered on top of each other before the centrifugation step. During ultracentrifugation, the particles migrate to the solution of identical density. If the separation were stopped at this point, it would be a non-equilibrium separation. If the separation is continued, however, the steps become continuous and an equilibrium separation can be obtained. Time required for an equilibrium separation can be decreased significantly by carefully choosing the concentration of each density step. Preformed discontinuous gradients are labor intensive, can require special equipment, and can be a source of inconsistency in the separation.

An ideal solute used for a density gradient separation would have a number of characteristics. Recent research has shown that cesium bismuth EDTA (CsBiY) and sodium bismuth EDTA (NaBiY) have many of the ideal properties for a density gradient forming solute (69).

There are several methods used for collecting and or measuring separated lipoproteins, such as fraction collection pumps (70,71,72), a tube cutting method (73), and pre-staining the lipoproteins and imaging the lipoproteins in the tube following separation (69,74,75,76,77). Utilizing digital photography improved the pre-staining/photographic method by making it possible to generate a density profile in much less time than other methods require. Also, photography is the only technique whose resolution depends only on the separation and not on the collection method. Dyes commonly used for lipoprotein analysis are either lipophilic or protein stains.

Fluorescence

Naturally occurring lipids, like the ones in lipoproteins, do not have chromophores that are suitable for many studies. Fluorescent probes have been utilized to study kinetic processes, cellular localization, and quantification of lipid classes. There are three main types of fluorescent probes used to study lipoproteins: lipid analogs, lipid-soluble dyes, and protein modifiers (78). Fluorescent probes can simplify experimental design when used properly.

Fluorescent phospholipid analogs have proven to be very useful in lipoprotein analysis because they incorporate themselves in the particle surface, and act much like a native phospholipid. Fluorescence measurements of suitably stained lipoprotein samples can detect low concentrations of lipoproteins without background interference. A widely used probe of this class is 7-nitrobenz-2-oxa-1,3-diazol-4-yl ceramide (NBD),

shown in Figure 9. Extensive studies have proven that NBD resides in the polar region of the lipoprotein (79,80).

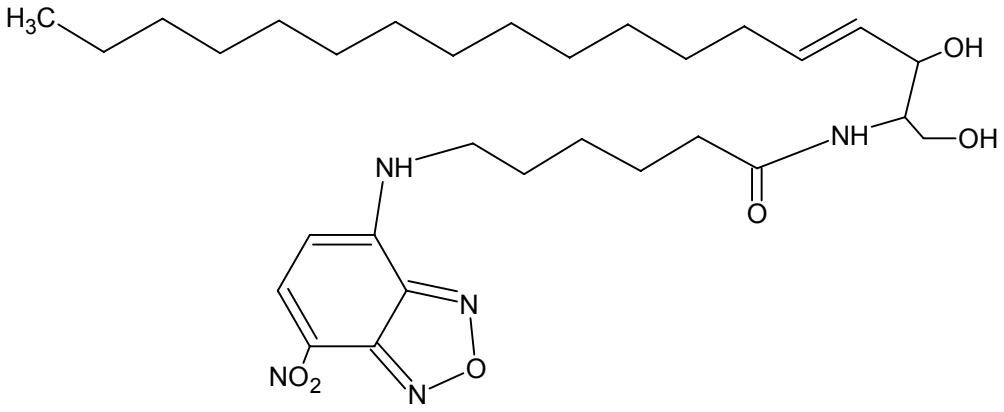

Figure 9. Structure of NBD.

It is thought that the hydrophilic domain in NBD causes it to loop back towards the surface of the membrane, where there exists a more polar environment. This phemonena also decreases the time necessary for lipoprotein staining. NBD has a large Stokes shift and broad absorption and emission peaks in the visible range (Figure 10). It is sensitive to the polarity of its environment, exhibiting a blue shift in emission wavelength maximum with decreasingly polar solvents (81). NBD staining can be used to quantitate the amount of lipoprotein in a sample (69), and is able to successfully stain lipoproteins when added to a serum sample (82).

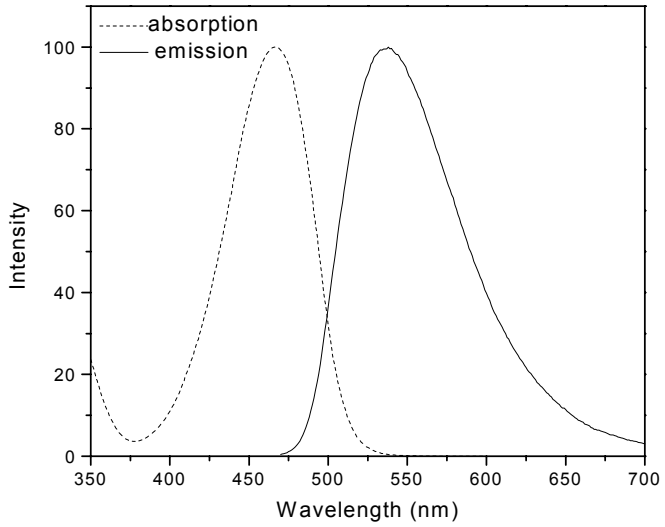

Figure 10. Absorption and emission spectra of NBD aminohexanoic acid in methanol (83).

Another fluorescent probe utilized in lipoprotein analysis is Nile Red (NR), also referred to in literature as 9-diethylamino-5H-benzo[α]phenoxazine-5-one, or Nile Blue A-oxazone (Figure 11). NR preferentially stains neutral lipids, such as cholesterol esters and triglycerides, and resides in the hydrophobic domain of the lipoprotein. Upon saturation of the lipid core, however, NR will interact with the surface lipids (84).

Unlike NBD, no literature cites the success of staining lipoproteins with NR by adding the probe to a serum sample. NR exhibits a large Stokes shift, and broad absorption and emission peaks (Figure 12).

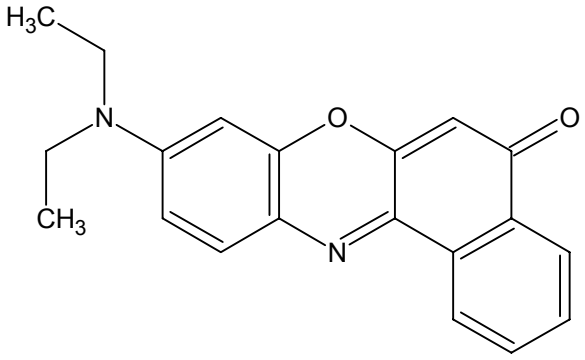

Figure 11. Structure of Nile Red.

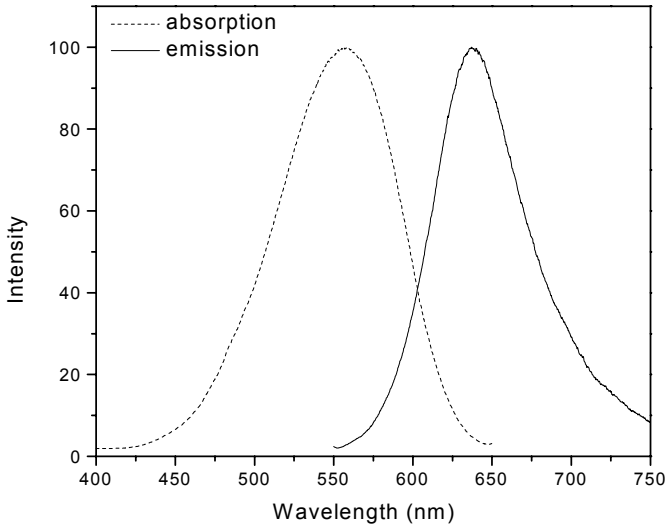

Figure 12. Absorption and emission spectra of Nile Red bound to a phospholipid bilayer membrane (85).

NR is a solvochromic dye, a probe whose absorption bands change in intensity, shape, and position depending on the polarity of the solvent (86). The excitation and emission maxima shift over a span of 100 nm when placed in solvents of differing

polarity (87). The shape of both the excitation and emission spectral curves changes as well, indicating specific solvent effects such as hydrogen bonding (87). Preliminary studies have shown perceptible changes in fluorescent profiles between native LDL and oxLDL, due to the differing lipid compositions of the particle. The oxLDL spectra are broader, and shifted to a longer wavelength (88). Acetylation of LDL only modifies the lysine residues and does not change the lipid composition. As expected, no change in NR fluorescence was observed between native and acetylated LDL (88).

Matrix-Assisted Laser Desorption/Ionization Time-of-Flight Mass Spectrometry

In 1988, Karas and Hillenkamp introduced a new ionization method for mass spectrometry of bioorganic compounds, especially non-volatile compounds, termed Matrix-Assisted Laser Desorption/Ionization (MALDI) (89). This soft ionization technique involves the use of a matrix, which consists of a solid that has a high absorbance in the ultraviolet region (90). A matrix has two major functions, absorption of the energy from an ultraviolet (UV) laser, and isolation of the sample molecules from each other (91). Following absorption of laser energy by the matrix, energy transfer to the sample molecules occurs in an efficient and controllable process. Analyte molecules are spared from excessive energy that would result in their decomposition. There is a low concentration of analyte molecules present in the matrix, and this dilution helps to prevent the sample molecules from associating with each other to form complexes with masses too large for desorption and analysis. The pulsed UV laser generates mostly singly-charged intact molecular ions, as well as dimers and doubly-charged molecular

ions (89,92,93). This ionization method is not completely understood, although it is probable that multiple reactions are occurring in the MALDI plume (93).

Time-of-flight (TOF) mass analyzers are often coupled to MALDI ion sources. In a TOF spectrometer, ions are accelerated to a fixed kinetic energy by an electrical potential. The velocity of the ions is proportional to $(m/z)^{-1/2}$, where m/z is the mass to charge ratio of the analyte ions (91,94). Ions then pass through a field-free region, where they are separated into groups of ions whose velocity is characteristic of their mass. A detector at the end of the field-free region produces a signal as each ion group strikes it, thus creating a mass spectrum.

The signal detected in the mass spectrum is highly dependent on the choice of matrix (91,93). Derivatives of cinnamic acid, such as sinapinic, ferulic, and caffeic acids, have proven to work satisfactorily for a range of proteins (95). Crystallization studies of sinapinic acid have shown that the protein molecule is incorporated into the crystal structure of the matrix (96).

Differing sample preparations can also affect the detected signal. The thin-layer method has been shown to produce homogenous spots for analysis. A spot of pure matrix is placed under the analyte and matrix sample. The spot can be washed with cold water to remove any contaminants from the crystallized structure. This method has increased sensitivity and resolution in comparison to other sample preparation methods (97).

MALDI-TOF-MS has been used successfully for the characterization of proteins. Complex protein mixtures can be elucidated because of the many singly-charged ions,

and high mass accuracy makes identification of individual proteins possible (91,98). Post-translational modifications, such as glycosylation and acetylation, can be easily detected with a MALDI-TOF-MS system (91,98). There are some drawbacks to protein analysis via MALDI-TOF-MS, such as suppression effects in the mass spectrum and possible differences in ionization efficiencies in the sample mixture.

Apolipoprotein mixtures have been characterized using MALDI-TOF-MS. HDL fractions have been analyzed for feasibility (99), as well as for characterization of novel isoforms of various apolipoproteins (100,101,102). VLDL fractions have been analyzed and new isoforms of apo C-III detected as well as polymorphisms of the apolipoproteins (100,103). Novel isoforms of apolipoproteins, believed to be products of methionine residue oxidation, have been detected in both VLDL and HDL fractions (100,104). Methionine residues in apo C-II and pro apo C-II are converted to either sulfoxides or sulfones, resulting in a mass shift of 16 or 32 Da respectively (100,101). Apo A-I has also been shown to undergo methionine oxidation (104,105,106,107). The detection of oxidation of apolipoproteins by MALDI-TOF MS has not been well established, however, so little more is known.

MATERIALS, INSTRUMENTATION, AND METHODS

Materials

Human Serum Collection

Serum samples were obtained by venipuncture into an 8 mL Vacuette® treated with silica clotting activator and containing a separation gel (Greiner Bio-One, Kremsmuenster, Austria).

Human Plasma Collection

Plasma samples were obtained by venopuncture into an 8 mL Vacuette® treated with lithium heparin and containing a separation gel (Greiner Bio-One, Kremsmuenster, Austria).

Sample Oxidation

Serum and plasma samples were oxidized using 2,2'-azobis-(2-amidinopropane) dihydrochloride (AAPH, 440914, Aldrich, Milwaukee, WI, USA) in eppendorf tubes (Eppendorf, Hamburg, Germany).

Thiobarbituric Acid Reactive Substances (TBARS) Assay

Oxidized samples were mixed with thiobarbituric acid (TBA, T-5500, Sigma, St. Louis, MO, USA) as a 0.4% (w/w) solution in deionized water from a Milli-Q water purification system (Millipore, Bedford, MA, USA), and 0.5% (w/w) butylated

hydroxytoluene (BHT, B-1378, Sigma, St. Louis, MO, USA) in acetic acid (99.7%, AX0073-9).

Separation of Lipoprotein Particle Classes by Single Spin Ultracentrifugation

A 20% (w/w) solution of cesium-bismuth-ethylenediaminetetracetic acid (EDTA) (CsBiY) in 0.02 M phosphate buffer (PB) was used as a density gradient for the separation of lipoprotein classes. The CsBiY was synthesized in our laboratory following a published procedure (108). The buffer was made from sodium phosphate monobasic (SX0710-1, EM Science, Gibbstown, NJ, USA) and dibasic (SX0715-1, EM Science, Gibbstown, NJ, USA) in a 1.6:1 ratio.

A 10% (w/v) solution of sodium-bismuth-EDTA (NaBiY) in water was also used as a density gradient. NaBiY is commercially available (E086, TCI America, Portland, OR, USA).

In either density gradient, serum and plasma samples were stained with N-(7-nitrobenz-2-oxa-1,3-diazol-7-yl)-6-ceramide (NBD, N-1154, Molecular Probes, Eugene, OR, USA) as a 1 mg/mL or 2 mg/mL solution in dimethyl sufoxide (DMSO, 99.9%, MX1458-6 Burdick &Jackson, Muskegon, MI, USA) or with Nile Red (N-1142, Molecular Probes, Eugene, OR, USA) as a 1 mg/mL solution in DMSO.

C_{18} Solid Phase Extraction, Desalting, and Delipidation

The proteins in VLDL, LDL, and HDL were delipidated and purified using a tC_{18} Light cartridge (Sep-Pack, 36805, Waters, Milford, MA, USA). Also used were

trifluoroacetic acid (TFA, T-6508, Sigma, St. Louis, MO, USA), and acetonitrile (ACN, 99.8%, AX0145-1, EM Science, Gibbstown, NJ, USA).

Matrix-Assisted Laser Desorption/Ionization Time-of-Flight Mass Spectrometry

Protein samples were prepared for MALDI-TOF-MS using sinapinic acid (98%, D-7927, Sigma, St. Louis, MO, USA) in methanol (99.8%, MX0475-1, EM Science, Gibbstown, NJ, USA) as a matrix.

Instrumentation

Serum and Plasma Collection

Serum and plasma were separated from red blood cells by a 3200 rpm centrifugation for 20 minutes at 4°C in a Compact II Centrifuge (Clay Adams Brand, Becton Dickinson, Franklin Lakes, NJ). Serum and plasma samples were divided into aliquots and stored at -85°C in a Revco Elite Freezer (Fisher Scientific, Pittsburgh, PA, USA) until analysis.

Sample Oxidation

Serum and plasma samples were oxidized by incubation at 37°C in an Isotemp Incubator (Model 5250, Fisher Scientific, Pittsburgh, PA, USA).

TBARS Assay

The TBARS assay constituents were incubated at 100°C in an Isotemp Vacuum Oven (Model 281, Fisher Scientific, Pittsburgh, PA, USA). Absorbance values were obtained on a μQuant Universal Microplate Spectrophotometer (Bio-tek Instruments, Inc., Winooski, VT, USA) using an acrylic 96 well UV-plate (Corning Costar, Acton, MA, USA).

Separation of Lipoprotein Particle Classes by Single Spin Ultracentrifugation

The separation of lipoprotein classes was achieved in a Beckman Optima TLX tabletop ultracentrifuge (UC) using a 30° fixed angle TLA 129.2 rotor (Beckman Instruments, Fullerton, CA, USA). Samples were placed in 1.5 mL open-top polycarbonate centrifuge tubes (Beckman Instruments, Fullerton, CA, USA).

Imaging and Analysis of UC Tubes

Imaging of the UC tubes containing sample stained with NBD occurred using a Nikon Coolpix 5000 camera (Nikon, Inc., Melville, NY) mounted in a custom built fluorescence photography station. In the system, the light source and camera were orthogonal to each other in order to minimize the amount of excitation light reaching the camera. The light source was a 50W halogen lamp (14927, General Electric Co., Cleveland, OH, USA). A hot mirror (46-452, Edmund Industrial Optics, Barrington, NJ, USA) and an excitation blue-pass glass filter (46-432, Edmund Industrial Optics, Barrington, NJ, USA) were placed between the light source and the sample chamber.

The camera was fitted with an emission dichroic Sybr Green filter (849 9246, Eastman Kodak, Rochester, NY, USA). The filters were chosen so that there was essentially no overlap in their band pass regions (Figure 13).

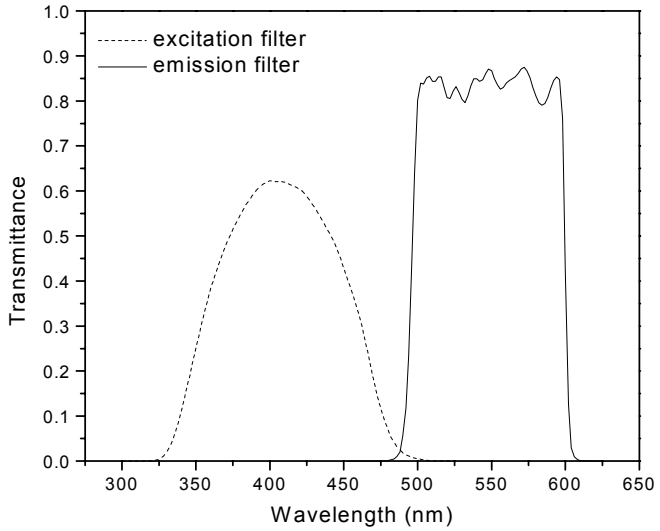

Figure 13. Transmittance curves for excitation and emission filters used with NBD.

UC tubes containing sample stained with NR were imaged on a different system. A 3.3 megapixel color digital Firewire System (Leica DFC 300, TM060769, Optronics, Goleta, CA, USA) was mounted on a composite bread board (19”X23”, Technical Manufacturing Corporation, Peabody, MA, USA) orthogonal to a fiber-lite metal halide machine vision illuminator (MH-100, Dolan Jenner Industries, Lawrence, MA, USA). Both used mounts from Edmund Industrial Optics (Barrington, NJ, USA), as did a custom built tube holder. The camera and light source were fitted with changeable

filters. The light source had a 400 nm bandpass excitation filter (46-431, Edmund Industrial Optics, Barrington, NJ, USA) and the camera had a 590 nm longpass emission filter (46-063, Edmund Industrial Optics, Barrington, NJ, USA) (Figure 14).

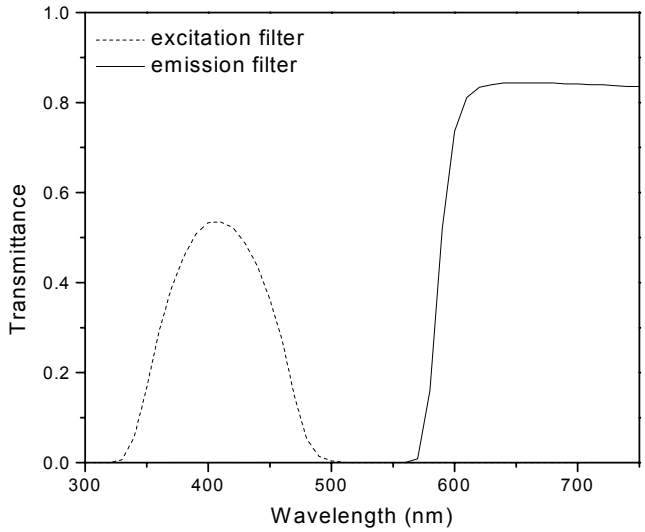

Figure 14. Transmittance curves for excitation and emission filters used with NR.

With either photography station, OriginPro7 (Microcal Software, Inc., Northampton, MA, USA) operated on a 650 MHz Pentium III computer was used for data analysis.

Fraction Collection

In order to collect lipoprotein fractions after the centrifugation step, a scroll saw (Model 1672, 16-inches, 2-speed, Dremel) with a thin blade (0.254 mm wide) was used to cut the centrifuge tubes. A custom brass template with built in micrometer assured accurate slicing. Sawdust was pelleted out of the lipoprotein fraction using a Minispin Plus centrifuge (Eppendorf, Hamburg, Germany).

Fluorescence Measurements

Fluorescence measurements were taken on a SLM Aminco Spectrofluorometer (Model 8100, Series 2, Spex, Jobin Yvon, Edison, NJ, USA). Samples were analyzed in the same polycarbonate tubes used for ultracentrifugation, held in position by a custom built holder.

C_{18} Solid Phase Extraction, Desalting, and Delipidation

For multiple analyses, a vacuum manifold (WAT200609, Waters, Milford, MA, USA) was used for cartridge delipidation and purification.

Matrix-Assisted Laser Desorption/Ionization Time-of-Flight Mass Spectrometry

MALDI-TOF-MS analysis was done using a commercial Voyager DE STR, equipped with a 2 meter flight tube (Applied Biosystems, Inc., Foster City, CA, USA).

Methods

Serum and Plasma Collection

All blood was taken from a normolipidemic subject following a 12 hour fast. Samples were collected via venopuncture at the Scott and White laboratory in College Station, TX. Serum or plasma was separated from red blood cells by centrifugation for 20 minutes at 3200 rpm at 4°C. The supernatant was removed, aliquoted, and stored at -85°C until analysis.

Sample Oxidation

In order to oxidize the sample, serum or plasma was mixed with 750 mM AAPH for a final AAPH concentration of 50 mM, and incubated at 37°C for times varying between six and 24 hours in closed eppendorf tubes. For 150 μL of serum, this equates to 10.7 μL of AAPH. Some later studies used a final AAPH concentration of 24 mM (150 μL of serum plus 5 μL of AAPH).

TBARS Assay

To measure the TBARS response, 50 μL of sample (oxidized or unoxidized serum or plasma) was mixed with 250 μL 0.4% (w/w) TBA solution in deionized water and 5μL 0.5% (w/w) BHT in acetic acid. The samples were incubated at 100°C for 20 minutes, and then pipetted into a 96-well plate. The absorbance spectrum was read from 500 to 600 nm, and an absorbance value read at 532 nm.

Separation of Lipoprotein Particle Classes by Single Spin Ultracentrifugation

The conventional method for separation of lipoprotein classes is density gradient centrifugation. A novel density gradient, CsBiY, was used to generate a self-forming density gradient upon ultracentrifugation. A 6 μL aliquot of serum was added to 590 μL of water, 600 μL 20% (w/w) CsBiY in 0.02 M PB, and 4 μL stain. The stain was one of two fluorescent probes, 1 mg/mL NBD or NR in DMSO. After complete mixing, 1 mL of sample was transferred to a clean ultracentrifuge tube. The tube was centrifuged for 4 hours 30 minutes at 120,000 rpm at 5°C.

NaBiY was also used as a density gradient. A 6 μL aliquot of serum was added to 1100 μL of 10% (w/v) NaBiY in water, and 4 μL 1 mg/mL NBD or NR in DMSO. After complete mixing, 1 mL of sample was transferred to a clean ultracentrifuge tube. The tube was centrifuged for 6 hours at 120,000 rpm at 5°C.

When more oxidized lipoprotein was necessary, a 60 μL aliquot of serum was added to 1100 μL of 10% (w/v) NaBiY in water, and 10 μL of 2 mg/mL NBD. Following complete mixing, 1 mL of sample was transferred to a clean ultracentrifuge tube, and was centrifuged for 6 hours at 120,000 rpm at 5°C.

Imaging and Analysis of UC Tubes

Following the ultracentrifugation step, each tube was photographed. The image was converted to a data file, and a density profile produced. Figure 15 shows an example of a lipoprotein profile. Profiles of unoxidized and oxidized samples were

compared, and the mean density of the LDL and HDL fractions calculated using a peak-fitting program.

Fraction Collection

Ultracentrifuge tubes were slowly frozen in liquid nitrogen following the UC spin and photography step. Individual lipoprotein fractions were collected by cutting the frozen tubes at specific cut positions calculated from the points of minimum fluorescence on the density profile, as shown in Figure 15. A thin blade scroll saw was utilized, as well as a custom built tube holder with micrometer to assure accurate cutting positions.

Following cutting, each fraction was centrifuged for 3 minutes at 7,000 g in order to remove any particulates remaining in the sample after the cutting step.

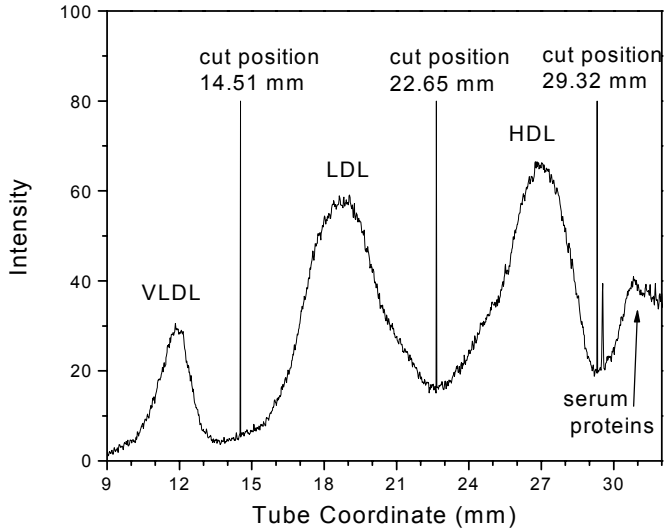

Figure 15. Lipoprotein density profile.

Fluorescence Measurements

For fluorescent analysis, fractions were placed in clean UC tubes. A custom built tube holder held the UC tubes in position in the spectrofluorometer. Emission and excitation scans were run on each sample. For samples stained with NBD, excitation scans were performed with the emission wavelength set at 536 nm, and emission scans done with the excitation wavelength of 466 nm. For samples stained with NR, excitation scans were performed with an emission wavelength set at 610, and emission scans done with an excitation wavelength of 535 nm.

C_{18} Solid Phase Extraction, Desalting, and Delipidation

A solid phase extraction cartridge was utilized to separate the apolipoproteins from the lipids in the lipoprotein particles. This delipidation process was based on a published method (109). The cartridge was first conditioned dropwise with 5 mL of 0.1% (v/v) TFA in acetonitrile, with no air being allowed to enter the cartridge. Next, the cartridge was conditioned dropwise with 5 mL 0.1% (v/v) TFA in water, again with no air being allowed to enter.

Samples were prepared for delipidation by adding 1% TFA in water until the final TFA concentration was 0.1%. Each sample was loaded slowly onto the cartridge.

Following sample loading, the cartridge was rinsed with 5 mL 0.1% (v/v) TFA in water in order to remove salts and contaminations from the UC spin. Air was pushed through the cartridge to remove any remaining liquid. Finally, proteins were eluted in 50 μL aliquots of 0.1% TFA in acetonitrile. The second, third, and fourth aliquots,

which contained the majority of the apolipoproteins, were collected and combined for further analysis.

Matrix-Assisted Laser Desorption/Ionization Time-of-Flight Mass Spectrometry

Protein samples were analyzed using a commercial MALDI-TOF mass spectrometer in the positive, linear mode. A thin-layer sample preparation method was used. A 0.5 μL aliquot of 35 mg/mL sinapinic acid was deposited on the plate and allowed to dry. Samples were prepared by mixing 2 μL of the eluted fraction with 3 μL of 25 mg/mL sinapinic acid and 6 μL deionized water. A 0.5 μL aliquot of the sample mixture was applied to the plate, and allowed to dry. Three 2 μL cold water rinses of the sample spot cleaned away any residual salt buildup. Mass spectra were calibrated using apolipoprotein A-I and apolipoprotein C-I.

RESULTS AND DISCUSSION

Optimization of *in Vitro* Oxidation of Lipoproteins as Monitored by the TBARS Assay

The first phase of this research was the investigation of the oxidation of lipoproteins. 2,2'-azobis-(2-amidinopropane) dihydrochloride (AAPH) was chosen as the oxidation initiator because of its frequent use in previous, well characterized, reproducible, lipoprotein oxidation studies.

The volume of serum needed for oxidation was considered. Literature cites large volumes of serum used for *in vitro* oxidation, up to 7 mL (53). A direct scale down study was carried out in order to adapt the method to a lower volume of 700 μL of serum. It was found that the high volume was unnecessary for the analyses following the oxidation step. Further experimentation showed that the volume of serum oxidized was directly proportional to the extent of oxidation when the AAPH concentration was held constant. In this study, the unoxidized sample was not incubated, but kept frozen at -85°C until analysis. Figure 16 illustrates the increase in TBARS response to decreasing serum volumes. Table 3 shows the TBARS response at 532 nm demonstrating this proportionality. Increased oxidation in lesser volumes is believed to be due to the diffusion control process. Smaller volumes allow for more diffusion and interaction to occur between particles, including the radicals initiated by AAPH.

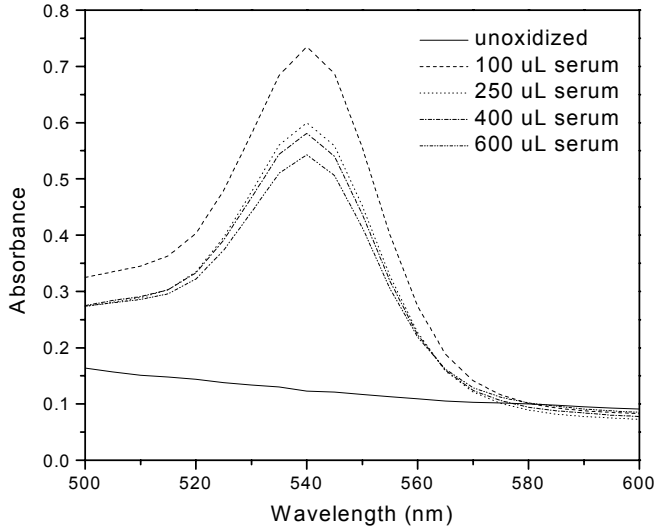

Figure 16. TBARS response to varying serum volumes with constant AAPH concentration. Oxidizing conditions were varying volumes of serum and 50 mM AAPH for 24 hours. Unoxidizing conditions were storage at -85°C.

Table 3. TBARS response to varying serum volume for oxidation, blanked with unoxidized serum. Conditions identical to those in Figure 16.

Volume oxidized serum (μL)	Absorbance at 532 nm
100 μL serum	0.506
250 μL serum	0.390
400 μL serum	0.378
600 μL serum	0.346

Once the volume of serum for oxidation was chosen, the incubation time at 37°C necessary to perceive oxidation was examined. For 100 μL of serum and an AAPH

concentration of 50 mM, minimal oxidation took place in the first hour of incubation. Figure 17 illustrates TBARS response over ten hours. After approximately five hours, the concentration of TBARS in the sample increased at a much slower rate (Figure 18). It was concluded that six hours is a satisfactory incubation time for the measurable oxidation of 100 μL of serum. Sample-to-sample relative standard deviation of the oxidation procedure was calculated to be 16.7% (n = 10), based on the TBARS assay.

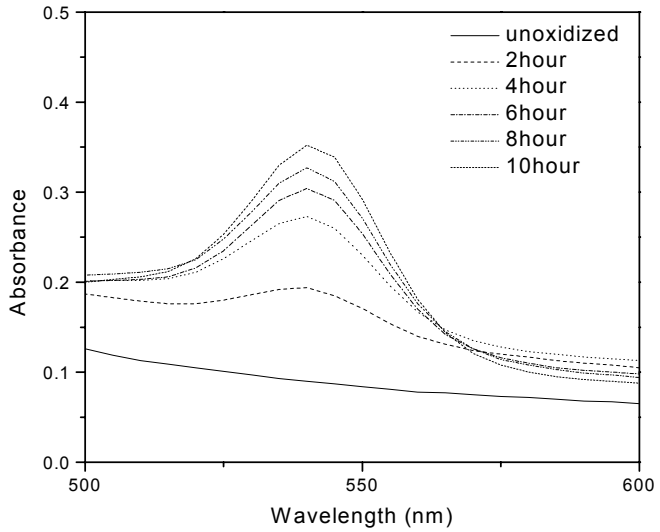

Figure 17. TBARS response to varying oxidation times. Oxidizing conditions were 100 μL of serum and 50 mM AAPH for varying times. Unoxidizing conditions were storage at -85°C.

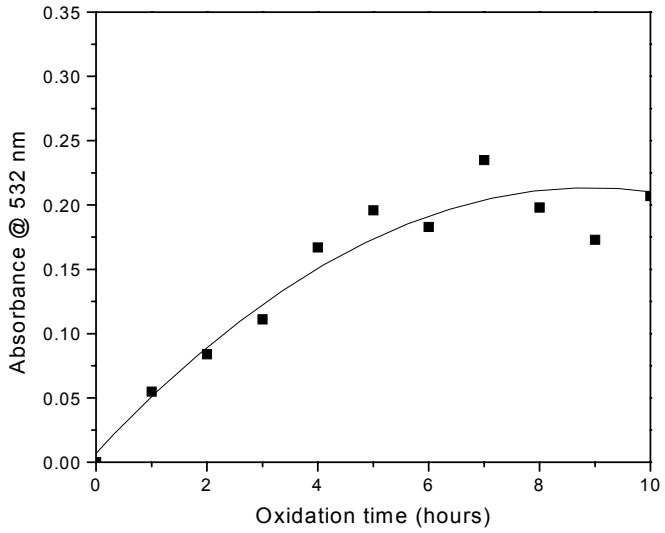

Figure 18. TBARS response to varying oxidation times, blanked with unoxidized serum. Conditions identical to those in Figure 17.

Initial estimates of how much oxidized serum was necessary for complete analysis were too low. Therefore, the volume of serum used in the oxidation step was increased to 150 μL. In order to increase the extent of oxidation of the lipoprotein particles, incubation time with AAPH was increased to 15 hours. Data confirmed that oxidation continued after 15 hours, indicating that the particle was not completely oxidized at the 15 hour time point.

TBARS Assay

During the development of the oxidation procedure it was necessary to adjust the TBARS assay protocol as well. Multiple procedures have been published for the

TBARS assay. For this research, however, a new TBARS procedure requiring only 50 μL of sample was developed.

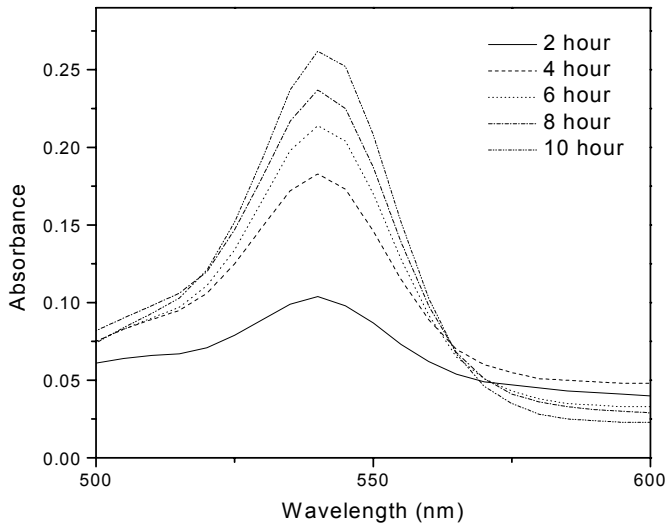

Figure 19. Absorbance vs wavelength of TBARS for varying oxidation times. Oxidizing conditions were 100 μL of serum and 50 mM AAPH for varying times.

A set of UV/Vis spectra from the TBARS assay over time of oxidation was recorded from 500 to 600 nm. A peak centered at 540 nm became more intense with time of oxidation (Figure 19). Literature cites the maximum of the TBARS chromophore at 532 nm; however experimentation in this study showed that the maximum lies at 540 nm. An experiment was performed to determine if absorbance measurements differed significantly between 532 nm and 540 nm. Results showed that

the two were very comparable; therefore, further measurements were obtained at 532 nm to comply with convention. Sample-to-sample standard deviation of absorbance measurements at 532 nm following the TBARS assay was calculated to be 2.57% (n = 5). Subsequent TBARS assays were performed as outlined in the Methods section (page 34).

Separation and Profiling of Lipoprotein Classes by Density Gradient Ultracentrifugation: Influence of Oxidation

The TBARS assay has many weaknesses, particularly specificity for elucidating lipid oxidation (60), and it was the goal of this research to develop a new detection technique for the susceptibility of lipoprotein oxidation. Our laboratory developed a density profiling method that is sensitive to slight shifts in the buoyant density of lipoprotein particles. Since oxidation of lipoproteins can change their properties, particularly density (17,40), the ultracentrifuge method was attractive for monitoring lipoprotein oxidation.

As oxidation occurs, low molecular weight oxidation products are formed in the lipid core and separate from the lipoprotein particle (17,37,40), causing a significant increase in buoyant density. These changes in the lipid core by exposure to AAPH were verified using the profiling procedure following the ultracentrifuge spin. Figure 20, Figure 21, and Figure 22 demonstrate that the shift in buoyant density over oxidation time closely shadows the response from the TBARS assay for lipid oxidation, indicating the density shift is indeed due to oxidation of the lipoprotein particles.

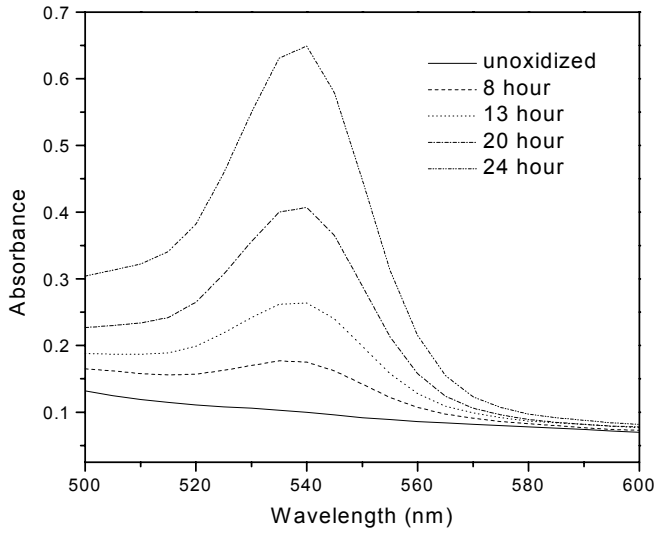

Figure 20. TBARS response over oxidation time. Oxidizing conditions were 700 μL of serum and 50 mM AAPH for varying times. Unoxidizing conditions were storage at -85°C.

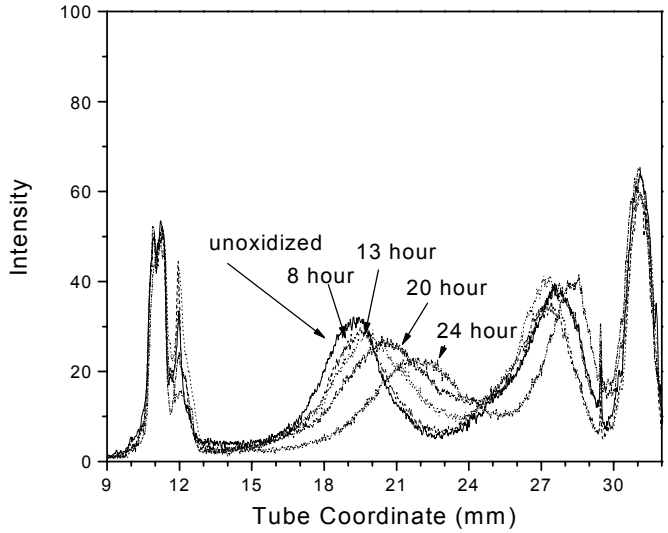

Figure 21. Buoyant density shift over oxidation time. Conditions identical to those in Figure 20. Ultracentrifuge conditions were NaBiY and NBD.

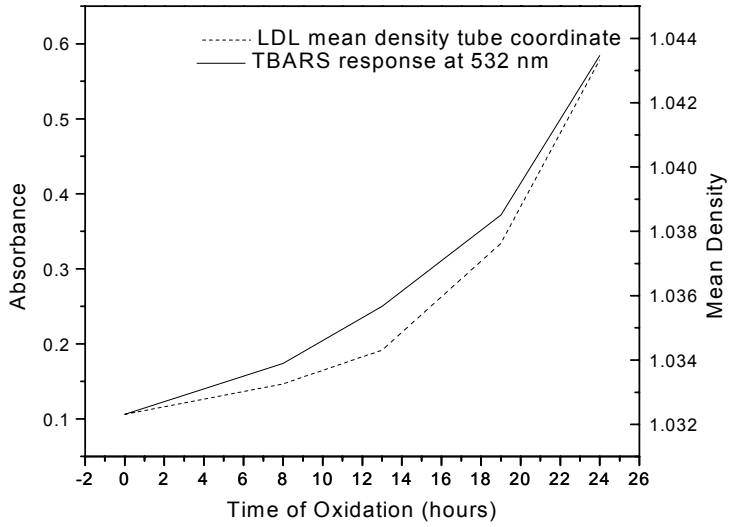

Figure 22. Comparison of TBARS response and LDL density shift. Conditions identical to those in Figure 20 and Figure 21.

As the incubation time increased, the mean buoyant density of the LDL particle also increased, indicating the loss of lipids and a higher protein to lipid ratio. LDL mean buoyant denisty shifted from 1.033 kg/L in the unoxidized sample to 1.043 kg/L in the 24 hour oxidized sample, a change of 0.010 kg/L (Figure 21). HDL also showed a shift in density as a function of oxidation time, from 1.088 kg/L in the unoxidized sample to 1.096 kg/L in the 24 hour oxidized sample. The change was 0.008 kg/L. The density gradient in the HDL is much steeper, and less movement is expected for an identical change in density. While peaks shift to a higher density, peak shape stays constant. This indicates that the entire population of particles is being oxidatively modified.

Influence of Fluorescent Probe on Lipoprotein Profiles

In the course of this research, two fluorescent probes were examined for their ability to document density profiles of individual lipoprotein classes. The first, 7-nitrobenz-2-oxa-1,3-diazol-4-yl ceramide (NBD), was highly successful in a CsBiY density gradient, as previously discussed (69), as well as in NaBiY. The NBD profile for unoxidizing and oxidizing conditions are shown in Figure 23.

Lower quality profiles were produced using the second probe, Nile Red (NR). In order to efficiently excite NR at its excitation wavelength, new filters were employed in the digital imaging system. The properties of these excitation and emission filters (Figure 14) are not ideal for the excitation and emission spectra of NR. The excitation filter does not completely overlap the excitation range of NR, resulting in less excitation energy reaching the fluorophore. This creates a non-zero baseline and contributes to the decrease in fluorescence intensity (Figure 24). Oxidized lipoproteins showed a significant density shift when stained with NBD (Figure 23), but the shift was considerably smaller when the same sample was stained with NR, an unexpected result. The mechanism of lipoprotein staining is, in general, not well understood. NR stains the core lipids of lipoproteins, which are the first to be oxidized (84). It is hypothesized that as oxidation occurs and alters the core of the lipoprotein particle, NR no longer has the same binding affinity. It stains the least oxidized lipoproteins preferentially, limiting the amount of buoyant density shift seen in the density profile.

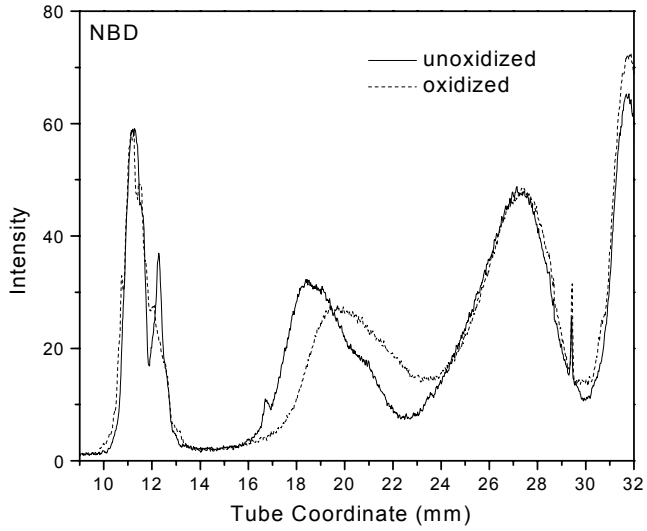

Figure 23. Density profile of lipoproteins stained with NBD in NaBiY. Oxidizing conditions were 100 μL of serum and 50 mM AAPH for six hours. Unoxidizing conditions were incubation at 37°C for six hours. Ultracentrifuge conditions were NaBiY and NBD.

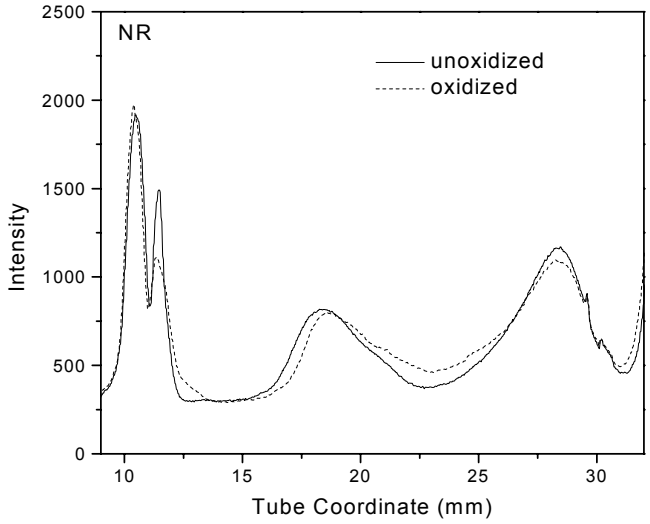

Figure 24. Density profile of lipoproteins stained with NR in NaBiY. Oxidizing and unoxidizing conditions were identical to those in Figure 23. Ultracentrifuge conditions were NaBiY and NR.

Influence of CsBiY vs NaBiY on Lipoprotein Profiles

NR does not fluoresce as intensely when in the presence of the NaBiY density gradient. Compared to the CsBiY, NaBiY resulted in a three-fold decrease in fluorescent intensity (Figure 25 and Figure 26). It is unclear why the fluorescence intensity is higher with CsBiY than with NaBiY. Similar studies with NBD exhibited a decrease in fluorescence intensity, however only a two-fold decrease was observed. The difference between NR and NBD properties in CsBiY and NaBiY is most likely due to their binding sites on the lipoprotein. NR binds in the hydrophobic lipid core, while NBD stays in the hydrophilic surface.

It can be hypothesized that the main difference between CsBiY and NaBiY is the sizes of the positively charged ions: Cesium ions (mw = 132.9) are much bigger than sodium ions (mw = 23.0). Lipoprotein particles are negatively charged, and the positively charged cesium and sodium ions are therefore attracted to it. Since the sodium ions are significantly smaller, they could pack more efficiently and shield the lipoprotein from interacting with the fluorescent probe. Cesium ions are larger, and cannot exert the same blocking action.

The loss of fluorescence intensity resulted in decreased detail in the lipoprotein peaks in the profiles. As shown in Figure 25, the LDL and HDL peaks are wide and not well resolved. It is difficult to determine where the LDL fraction ends and HDL begins, and there is no evidence of the detail that can be seen with NR in CsBiY (Figure 26), or with NBD in NaBiY (Figure 23). NaBiY was the medium of choice because it is commercially available and gives comparable profiles to CsBiY when NBD is used.

The combination of NaBiY and NBD was determined to be a more efficient system for lipoprotein profiling than NaBiY and NR. Therefore, NBD was used for further density shift experiments.

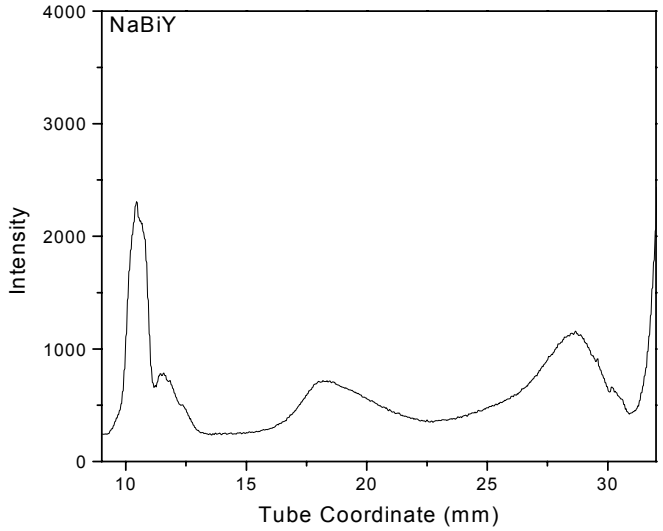

Figure 25. Density profile of unoxidized lipoproteins stained with NR in NaBiY.

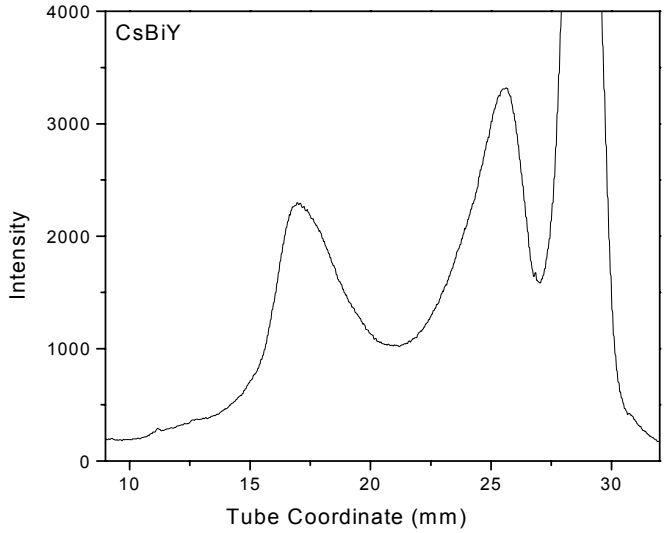

Figure 26. Density profile of unoxidized lipoproteins stained with NR in CsBiY.

Influence of Serum vs Plasma on Lipoprotein Profiles

Human serum and plasma were examined, as they are both used in lipoprotein oxidation studies reported in literature, to determine whether serum or plasma should be used in the study. In time-dependent oxidation studies, density profiles of the two sample types were almost identical (Figure 27 and Figure 28). Serum was chosen for further studies in order to mainstream the procedures, as well as to provide consistency with previous results obtained in our laboratory.

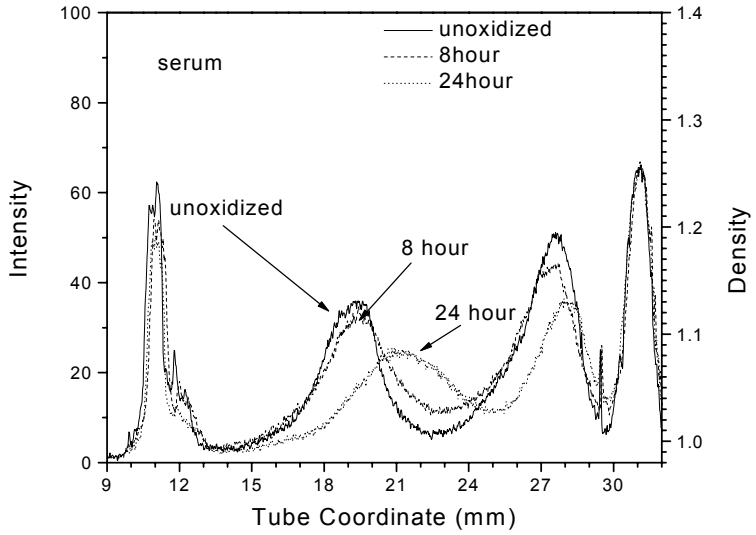

Figure 27. Density profile of serum. Oxidizing conditions were 650 μL of serum and 50 mM AAPH for 24 hours. Unoxidizing conditions were storage at -85°C for 24 hours. Ultracentrifuge conditions were CsBiY and NBD.

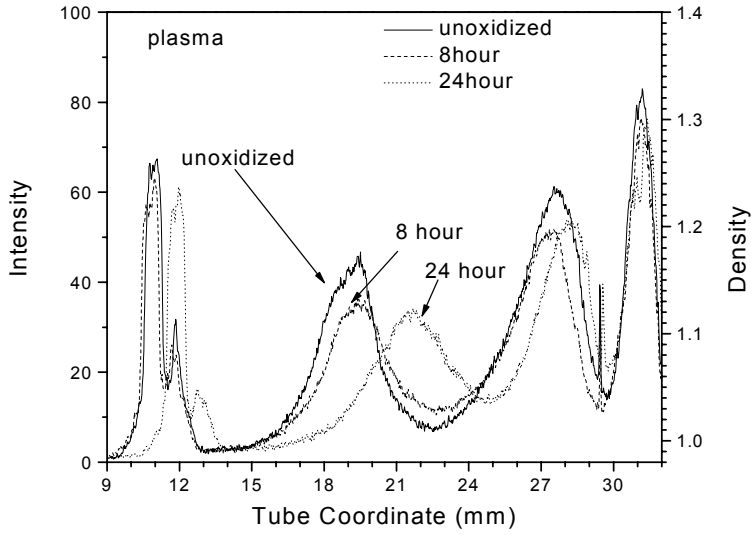

Figure 28. Density profile of plasma. Oxidizing conditions were 650 μL of serum and 50 mM AAPH for 24 hours. Unoxidizing conditions were storage at -85°C for 24 hours. Ultracentrifuge conditions were CsBiY and NBD.

Influence of 37°C Incubation on the Lipoprotein Profiles of Control Samples

Two kinds of unoxidized control samples were studied. The first was incubated at 37°C for the same amount of time as the oxidized sample being studied. No AAPH was added, and presumably no oxidation took place. The second control was kept at -85°C during the incubation step for the oxidized samples, and then thawed for analysis. For a 24 hour incubation the TBARS assay showed little difference between the two controls (Figure 29), indicating no oxidation took place without AAPH. The density profiles, however, were distinctly different (Figure 30). A hypothesis is that during incubation, surface lipids are shed from the lipoprotein particle, thereby changing its density. TBARS response would not change, as the freed lipids are unoxidized.

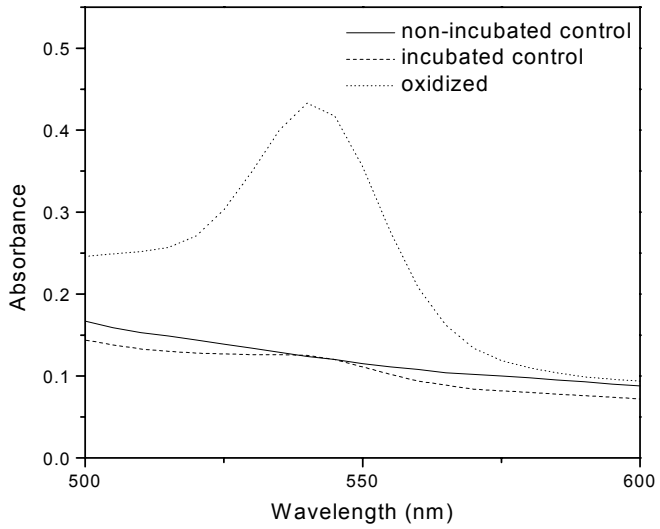

Figure 29. TBARS of non-incubated and incubated controls. Oxidizing conditions were 650 μL of serum and 50 mM AAPH for 24 hours. Unoxidizing conditions were storage at -85°C or incubation at 37°C for 24 hours.

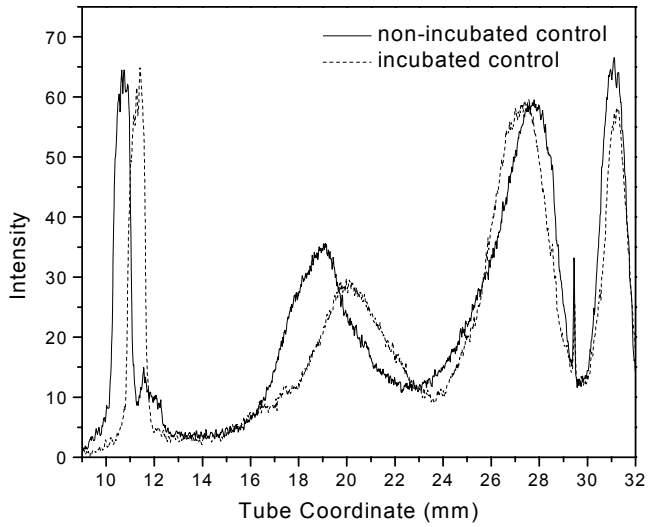

Figure 30. Density profiles of non-incubated and incubated controls in CsBiY. Conditions identical to those in Figure 29. Ultracentrifuge conditions were CsBiY and NBD.

When sample volume was decreased to 150 μL and incubation time decreased to 15 hours, the density profiles for the two controls showed no mean density shifts in the lipoprotein particles (Figure 31). No process in the incubation step was affecting the density profile.

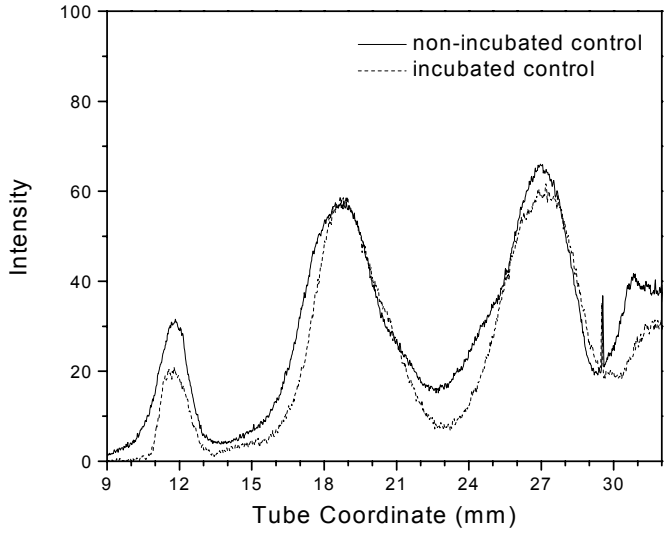

Figure 31. Density profiles of non-incubated and incubated controls in NaBiY. Unoxidizing conditions were storage of 150 μL of serum at -85°C or incubation at 37°C for 15 hours. Ultracentrifuge conditions were NaBiY and NBD.

Influence of Serum Volume on Lipoprotein Profiles

The influence of volume of serum used in the ultracentrifuge step was investigated by examining 6 μL and 60 μL samples. Both produced acceptable lipoprotein profiles; however, the 60 μL volume was shown to give a more intense

fluorescence signal and have higher sample-to-sample reproducibility. Based on this result, further work was carried out using the 60 μL serum sample.

Fluorescent Probe Analysis

Both fluorescent probes used in the density profiling step are sensitive to their microenvironment. As the polarity of their surroundings increase, the absorption and emission maxima of the probes shift to a higher wavelength. The use of this shift for the detection of oxidation was investigated using UC fractions.

NBD stained lipoproteins exhibited no shift in the absorption or emission between oxidized and unoxidized serum samples in either the LDL (Figure 32) or HDL (data not shown). This observation could be due to the fact that the NBD stain is not sensitive to minor environmental changes such as oxidation. The NBD resides on the surface of the lipoprotein, in the hydrophilic domain (79,80), whose constituents are only oxidized after the lipid core has been completely oxidized (110). The fact that no shift in wavelength maxima was detected may be due to the location of the NBD fluorophore in the lipoprotein particle.

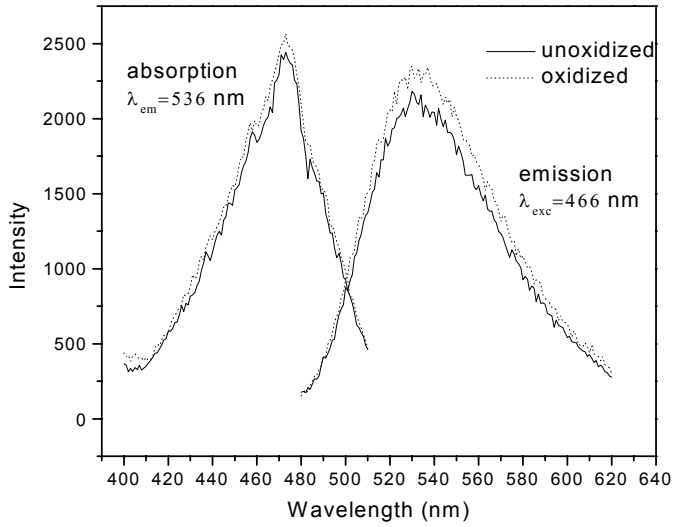

Figure 32. Absorption and emission spectra for NBD labeled LDL.

A shift was detected in both absorbance and emission peaks for the NR stained LDL and HDL. The LDL emission peak shifted from 608 nm in the unoxidized sample to 616 nm in the oxidized sample, and the excitation peak shifted from 505 nm to 526 nm (Figure 33). HDL fractions did not exhibit shifts as large as those seen in LDL. Emission shifted from 621 nm to 622 nm and excitation from 523 to 529 (Figure 34).

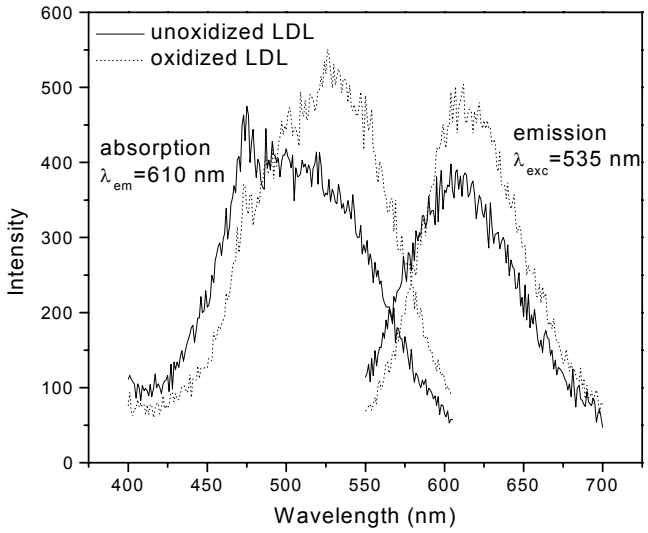

Figure 33. Absorption and emission spectra for NR labeled LDL.

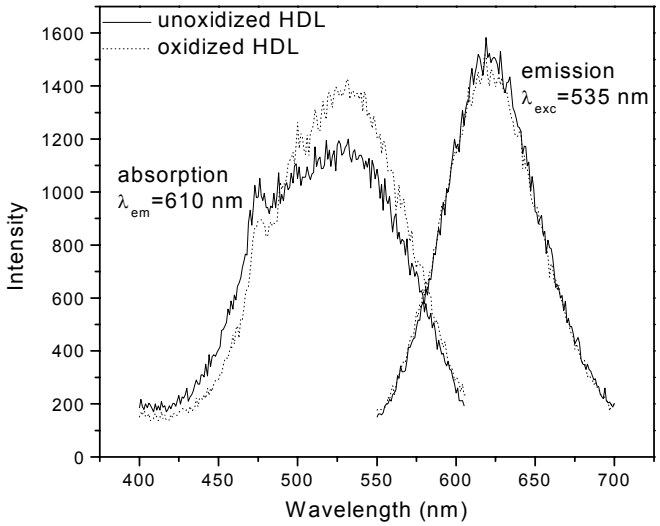

Figure 34. Absorption and emission spectra for NR labeled HDL.

An interesting result was that NR had different absorption and emssion peak maxima for unoxidized HDL and LDL, reflecting the different microenvironments of the lipoprotein particles. Both the absorption and emission peaks for the HDL were centered at higher wavelengths than those for LDL, indicating a more polar environment in the HDL particle. This observation makes sense due to the fact that LDL contains a higher proportion of non-polar lipids than does HDL.

In the excitation spectra, each LDL and HDL peak has a shoulder at 475 nm. Because the shoulder appears in both oxidized and unoxidized samples, it was assumed not to be a product of the oxidation step. The exact identity of this chromophore is unclear, however it could be used as an internal calibrant for fluorescence measurements due to its consistent presence.

While shifts in the absorption and emission spectra due to oxidation were observed, the most sensitive markers for oxidation were found to be the density profile and MALDI-TOF-MS of the HDL apolipoproteins.

MALDI-TOF-MS

As lipoproteins undergo oxidation, lipid moieties are changed as well as protein moieties. Changes in lipoprotein lipid content are observed by mean density shifts in the density profile, which is especially useful for LDL modifications. HDL consists of many lipoprotein particles whose oxidative modifications could be studied using MALDI-TOF-MS. The apolipoproteins in HDL are of mass ranges suitable for MALDI

analysis, and the method is sensitive enough to elucidate small mass changes due to oxidative processes.

Two control samples were analyzed, one not incubated (Figure 35), and the other incubated at 37°C for 15 hours (Figure 36). The only difference between the two spectra was the appearance of a truncated isoform of SAA_4 (SAA_4''') in the incubated sample. Addition of AAPH without incubation (no oxidation) showed no significant differences in peak appearance or m/z values compared to the unoxidized samples (data not shown). Thus, any changes in the spectra could be attributed to either incubation or AAPH oxidation. Furthermore, two samples of varying levels of oxidation were studied. The lesser oxidized sample was incubated with 24 mM AAPH (Figure 37), and the more oxidized sample incubated with 50 mM AAPH (Figure 38) for the same 15 hour period.

The control samples were very similar to previously recorded spectra of unoxidized HDL (102). Several significant changes were easily observed in the oxidized spectra. In the lesser oxidized sample, a new peak was formed at 13870 m/z. The isoforms of SAA_4 shifted in distribution. A second new peak was formed 800 m/z higher than apo A-I, and the A-I dimer completely disappeared. The more oxidized sample illustrated all these changes, as well as the apo C-I and apo C-I' peaks splitting into doublets.

Observed m/z values for oxidized and unoxidized samples, as well as calculated values, can be found in Table 4. Table 5 summarizes the differences between oxidized and unoxidized spectra.

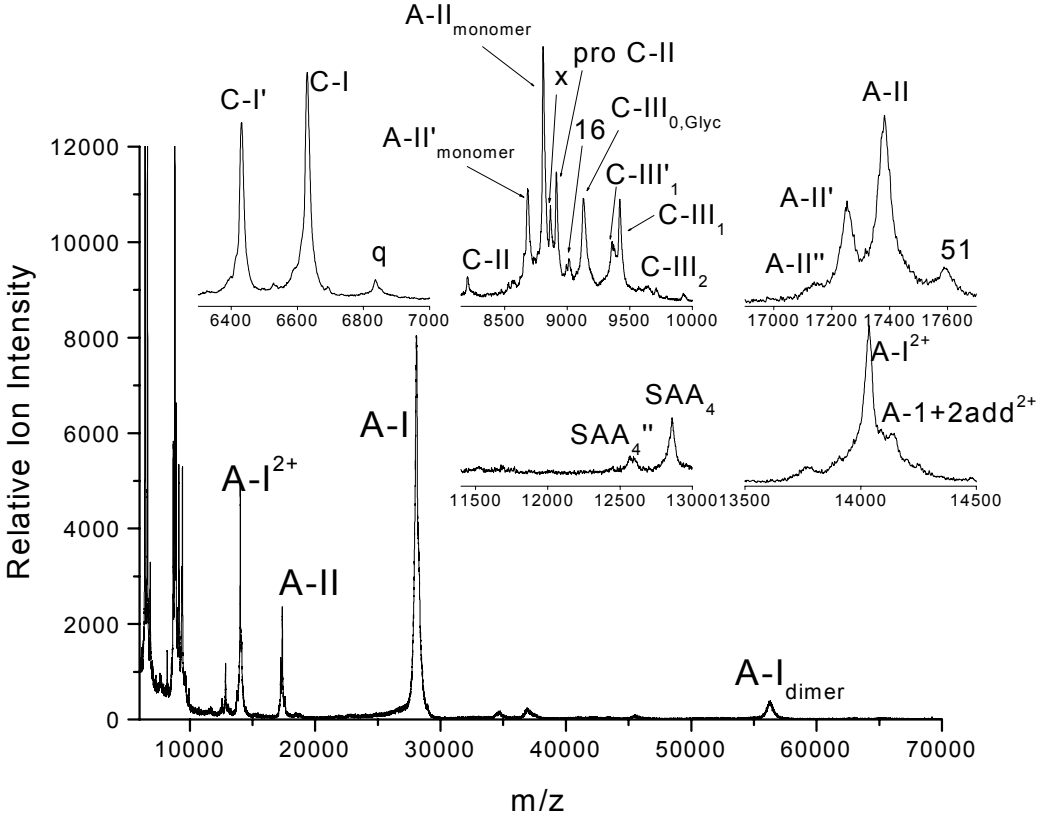

Figure 35. MALDI mass spectrum of apolipoproteins from non-incubated HDL.

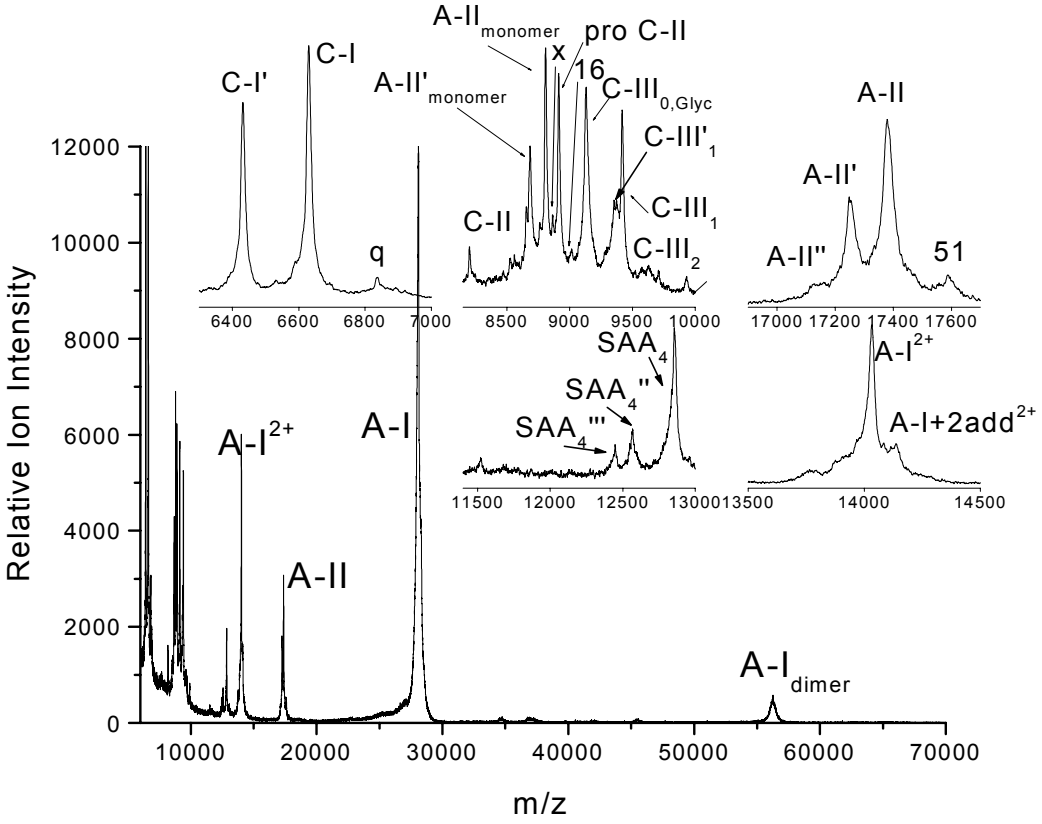

Figure 36. MALDI mass spectrum of apolipoproteins from incubated HDL.

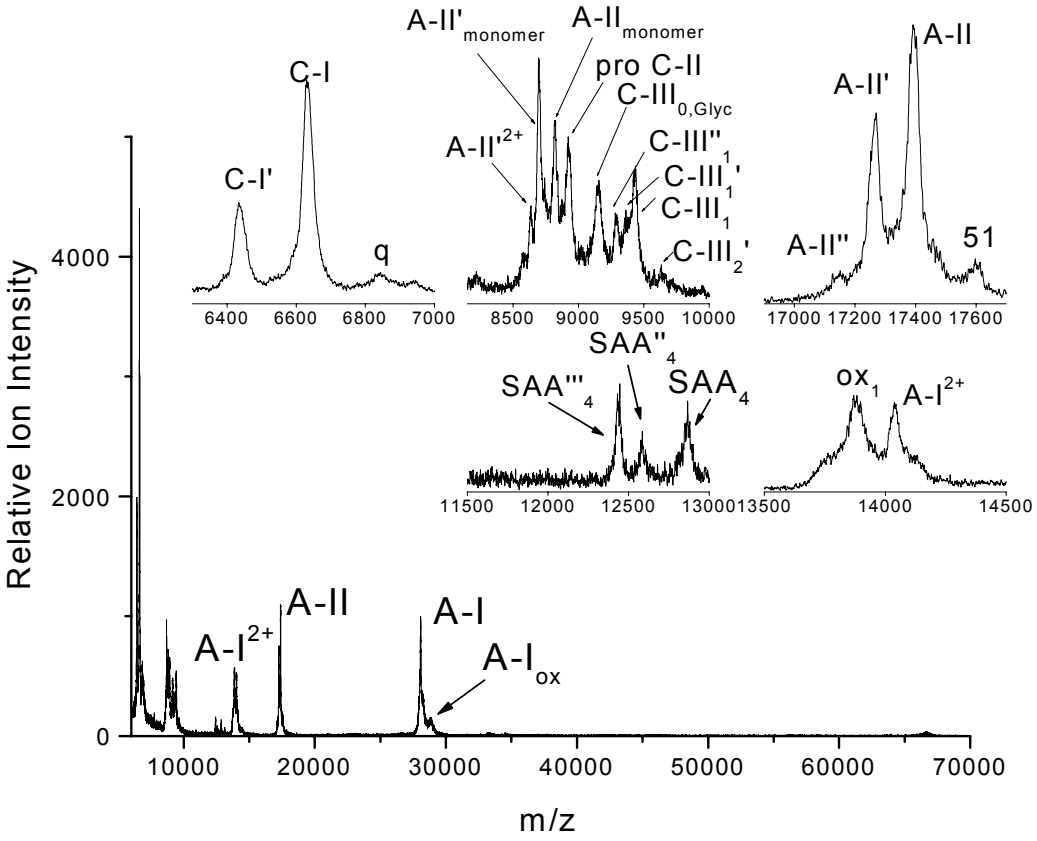

Figure 37. MALDI mass spectrum of HDL oxidized with 24 mM AAPH for 15 hours.

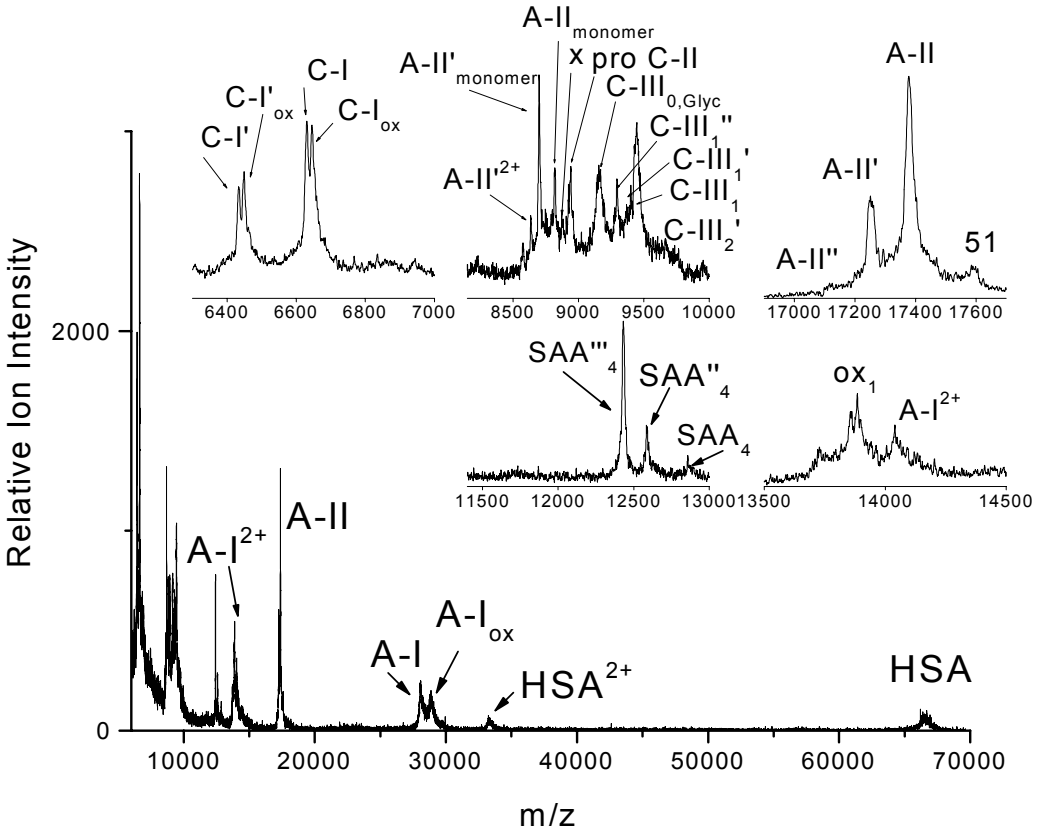

Figure 38. MALDI mass spectrum of HDL oxidized with 50 mM AAPH for 15 hours.

Table 4. Identification of peaks in mass spectra of HDL fractions.

Average $Mass_{unox}$	Average $Mass_{ox}$	MW calc	Code	Identification
6426.43	6435.94	6432.40	C-I'	Apo C-I minus N-Thr-Pro
-	6448.35	6448.40	C-I'$_{ox}$	Oxidized Apo C-I', + 16 Da
6630.60	6630.60	6630.60	C-I	Apo C-I
-	6646.04	6646.60	C-I$_{ox}$	Oxidized apo C-I, + 16 Da
6844.85	6831.87	6836.80	q	Apo C-I + 206 Da adduct
8208.44	-	8204.10	C-II	Apo C-II
-	8635.25	8626.85	A-II'$^{2+}$	Apo A-II minus C-Gln-Gln, z = 2
8684.26	8699.16	8681.80	A-II'$_{monomer}$	Apo A-II$_{monomer}$ minus C-Gln
8809.11	8819.30	8809.90	A-II$_{monomer}$	Single chain apo A-II
8870.70	8883.13	-	x	Unidentified
8913.15	8922.81	8914.90	pro C-II	pro Apo C-II
9018.55	-	-	16	A-II$_{monomer}$ + 209 Da adduct
9132.62	9143.37	9130.00	C-III$_{0,Glyc}$	Galβ1,3GalNAc-O-C-III$_0$
-	9288.21	9279.10	C-III$_1$''	Apo C-III$_1$ minus C-Ala-Ala
9363.28	9360.75	9350.20	C-III$_1$'	Apo C-III$_1$ minus C-Ala
9419.65	9427.84	9421.30	C-III$_1$	Apo C-III$_1$
9580.81	9572.29	9570.40	C-III$_2$''	Apo C-III$_2$ minus C-Ala-Ala
9641.56	9636.52	9641.50	C-III$_2$'	Apo C-III$_2$ minus C-Ala
9718.39	-	9712.60	C-III$_2$	Apo C-III$_2$
12451.56	12456.41	12443.60	SAA$_4$'''	SAA$_4$ minus C-Lys-Lys-Tyr
12571.28	12587.36	12571.80	SAA$_4$''	SAA$_4$ minus C-Lys-Tyr
12857.56	12862.24	12863.20	SAA$_4$	SAA$_4$
-	13869.73	-	ox$_1$	Unidentified oxidation product
-	13941.05	13881.20	A-I''$^{2+}$	Apo A-I minus C-Thr-Gln
14033.73	14039.03	14039.30	A-I^{2+}	Apo A-I, z = 2
14139.58	14153.13	14137.40	A-I+2add^{2+}	Apo A-I + 2-98 Da, z = 2
-	14465.33	14480.80	pro A-I^{2+}	pro Apo A-I, z = 2
17146.31	17135.42	17125.60	A-II''	Apo A-II minus 2-C-Gln
17254.61	17258.93	17253.70	A-II'	Apo A-II minus C-Gln
17381.78	17386.67	17379.80	A-II	Apo A-II
17596.33	17599.41	-	51	Unidentified
28078.60	28078.60	28078.60	A-I	Apo A-I
-	28851.35	-	A-I$_{ox}$	Unidentified (A-I ox peak,+800)
-	33353.29	33000.00	HSA^{2+}	Albumin, z = 2
56265.90	-	56157.20	A-I$_{dimer}$	A-I dimer
-	66680.99	66000.00	HSA	Albumin

Table 5. Differences in unoxidized and oxidized MALDI-TOF mass spectra.

- Apo C-I' and apo C-I form new peaks, 16 Da higher than the parent
- 10 m/z increase in proapo C-II
- 11 m/z increase in apo C-$III_{0,Gly}$
- Isoform distribution of SAA_4, SAA_4'', and SAA_4''' reverses in intensity
- 16 m/z increase in SAA_4''
- 10 m/z increase in apo A-$II_{monomer}$
- Apo A-I forms a new peak, 800 Da higher than the parent
- New peak at 13870 Da

The mass spectrum for an oxidized sample is significantly different from one for an unoxidized sample. Apolipoprotein C-I (apo C-I) is involved in the activation of lecithin:cholesterol acyltransferase (LCAT) (111,112), an enzyme whose main function is the conversion of cholesterol to cholesterol ester (113). A truncated form of apo C-I, apo C-I', has been identified as lacking two amino acid residues from the N-terminus as determined by MALDI-TOF-MS (114). Apo C-I' and C-I appeared as singlets in both unoxidized spectra as well as the least oxidized sample. However, after further oxidation, both the apo C-I' and apo C-I appeared as doublets differing in m/z by 16 Da. This change is expected due to the conversion of the protein's single methionine residue to a sulfoxide.

Apolipoprotein C-II (apo C-II) exists as two isoforms, mature apo C-II and proapo C-II (114). This protein activates lipoprotein lipase (115,116), which catalyzes the hydrolysis of triglycerides (117). Apo C-II did not exhibit any changes upon oxidation; however the molecular weight of proapo C-II increased by 10 m/z units.

The region from 8500 to 10,000 m/z changed significantly dependent on oxidation. An increased number of peaks are present as well as a higher baseline, indicating the probable presence of an increased number of ion species in that region.

Apolipoprotein C-III (apo C-III) plays a significant role in triglyceride metabolism (118). Apo C-III is found in serum as three isoforms, apo $C\text{-}III_o$, apo $C\text{-}III_1$, and apo $C\text{-}III_2$, differentiated by their degree of sialylation (118). Following oxidation, the $C\text{-}III_{0,Gly}$ peak appeared at a m/z ratio 11 Da higher than the unoxidized samples. No change was observed in the other apo C-IIIs.

Serum amyloid A (SAA) is an acute-phase protein of unknown function that exists in six isoforms (119,120). SAA_4 is found in normal serum (121), and has three distinct isoforms, SAA_4''', SAA_4'', and SAA_4 (102). In unoxidized serum, the most dominant peak is SAA_4, followed by the truncated forms SAA''_4 and SAA'''_4. In the oxidized state, SAA'''_4 is the dominant peak, followed by SAA''_4 and SAA_4. This reversal of isoform dominance in the mass spectrum implies that oxidation may contribute to the shedding of amino acids from intact SAA_4. Another interesting note is that the SAA''_4 m/z increases by 16 from the unoxidized to the oxidized samples. There are two methionine residues in SAA, and the m/z change could be due to sulfoxide formation.

Apolipoprotein A-II (apo A-II) is important to the structure of lipoproteins due to its lipid binding characteristics (118). Apo A-II exerts a negative influence on reverse cholesterol transport, promoting the development of atherosclerosis (111,122,123). In serum, apo A-II exists as a dimer, joined by a disulfide bond. Some oxidation methods,

such as performic acid oxidation, break this bond, resulting in a complete loss of the apo A-II dimer peaks in the mass spectrum (100,101). It was found that AAPH oxidation, however, does not break the disulfide link because peaks are present at the m/z for the A-II dimers. Peaks are also located at the m/z for apo A-II monomer in both unoxidized and oxidized samples. Oxidized samples show no doublet structure; however the m/z ratio for the apo A-II monomer is 10 m/z units higher than the unoxidized samples.

Apolipoprotein A-I (apo A-I) is the main protein in HDL, and is an important structural component of lipoproteins (118). Apo A-I is released into serum in a non-mature state (proapo A-I), followed by cleavage of six amino acid residues to form the mature protein. One of the major functions of apo A-I is the activation of LCAT (111). Apo A-I in unoxidized samples is observed as a singlet, but in oxidized samples it appears as a wide doublet, differing by a m/z of ~800 Da. The exact nature of the modifications that occur to the apo A-I molecule during oxidation are not yet known. Another new peak is observed 169 m/z less than the apo A-I^{2+} peak. Apo A-I^{2+} does not exist in serum; it is only present as an ion during the MALDI process. This new peak cannot be an oxidized form of apo A-I^{2+}; however its identity is unknown.

CLINICAL APPLICATION

The methods developed in this research were applied to a pilot clinical study involving the role of California grapes as a source of dietary antioxidants. Initial scientific interest in grapes stemmed from the French Paradox, an epidemiological study that found certain populations in France to have a high intake of saturated fats and relatively high plasma cholesterol, yet a low coronary heart disease mortality rate (124). This paradox has been partially attributed to a routine consumption of wine. Phenolic substances in grapes act as potent antioxidants. However the phenolic profile of wine differs from that of fresh grapes, as the grape crushing step and wine fermentation and aging cause significant changes in phenolic composition. Table grapes, or grapes meant to be consumed fresh, have also been shown to significantly inhibit LDL oxidation *in vitro* (125,126). The California Table Grape Commission has developed a freeze-dried grape powder that conserves the integrity of biologically active compounds found in fresh grapes. This powder can be used for *in vivo* or *in vitro* studies on the antioxidant effects of grape phenolic compounds.

A volunteer ate foods low in phenolic compounds for 24 hours followed by a 12 hour fast. A baseline blood sample was drawn, followed by the consumption of the equivalent of five servings of table grapes in a freeze-dried powder provided by the California Table Grape Commission. Blood was drawn each hour for five hours following grape consumption.

The six samples were oxidized with AAPH and separated using the ultracentrifugation spin with fluorescent NBD stain. A control that remained frozen during the oxidation step was also included. Density profiles were constructed for each sample, and mean buoyant density values for LDL and HDL were determined using a peak-fitting program. HDL fractions were isolated by cutting the tube at positions determined by the minima between classes. Apolipoproteins were purified by tC_{18} Light cartridge delipidation, and MALDI-TOF-MS analysis was performed. Figure 39 through Figure 52 show the density profiles and MALDI spectra for the samples. Mean density values and tube coordinates are indicated in the profiles

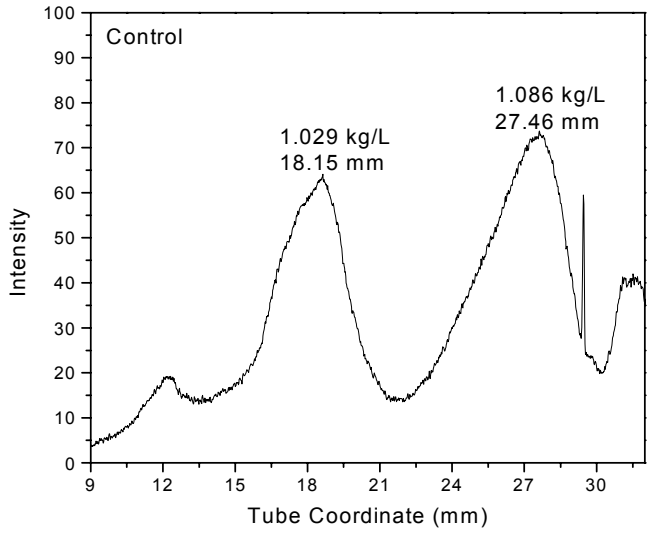

Figure 39. Density profile of control sample.

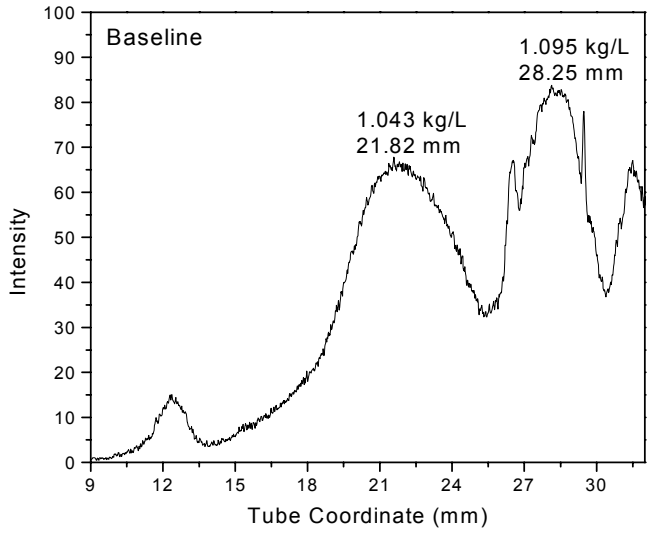

Figure 40. Density profile of baseline sample.

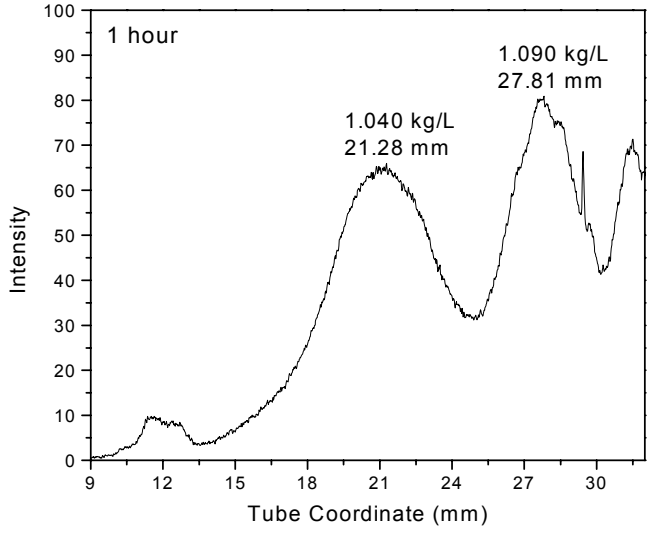

Figure 41. Density profile of one hour sample.

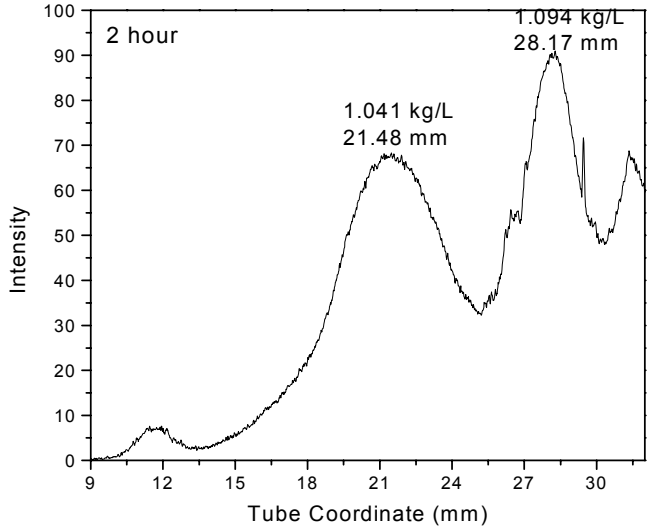

Figure 42. Density profile of two hour sample.

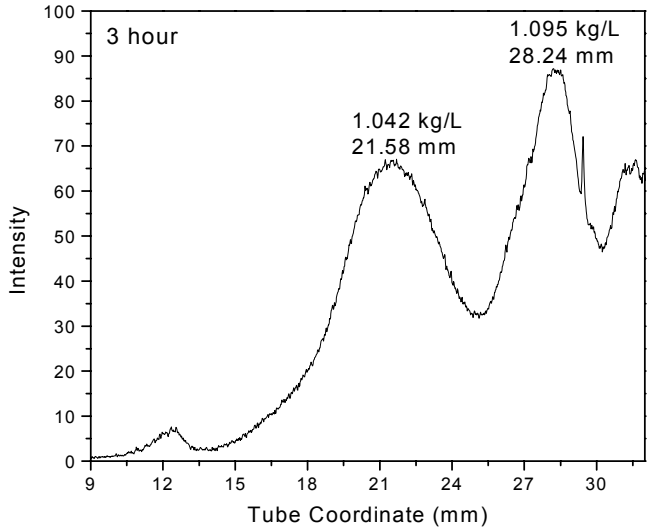

Figure 43. Density profile of three hour sample.

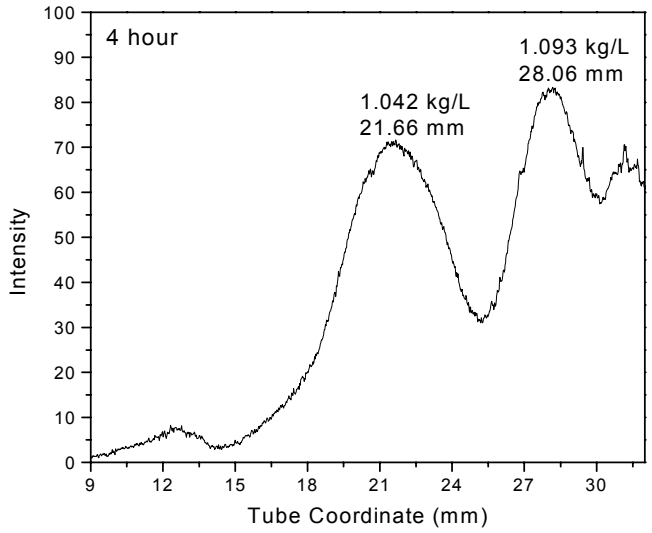

Figure 44. Density profile of four hour sample.

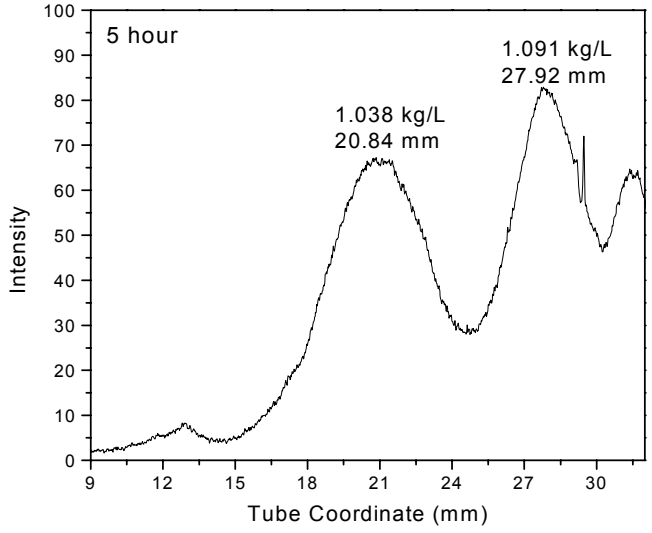

Figure 45. Density profile of five hour sample.

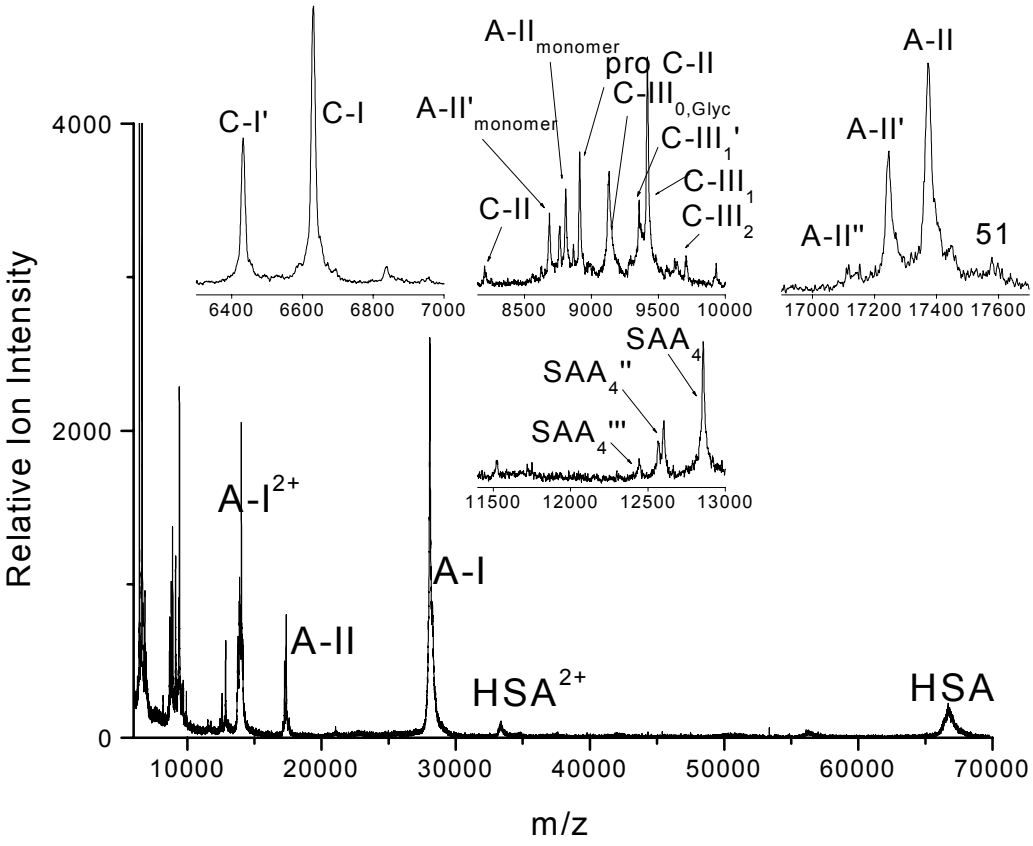

Figure 46. MALDI-TOF analysis of control sample.

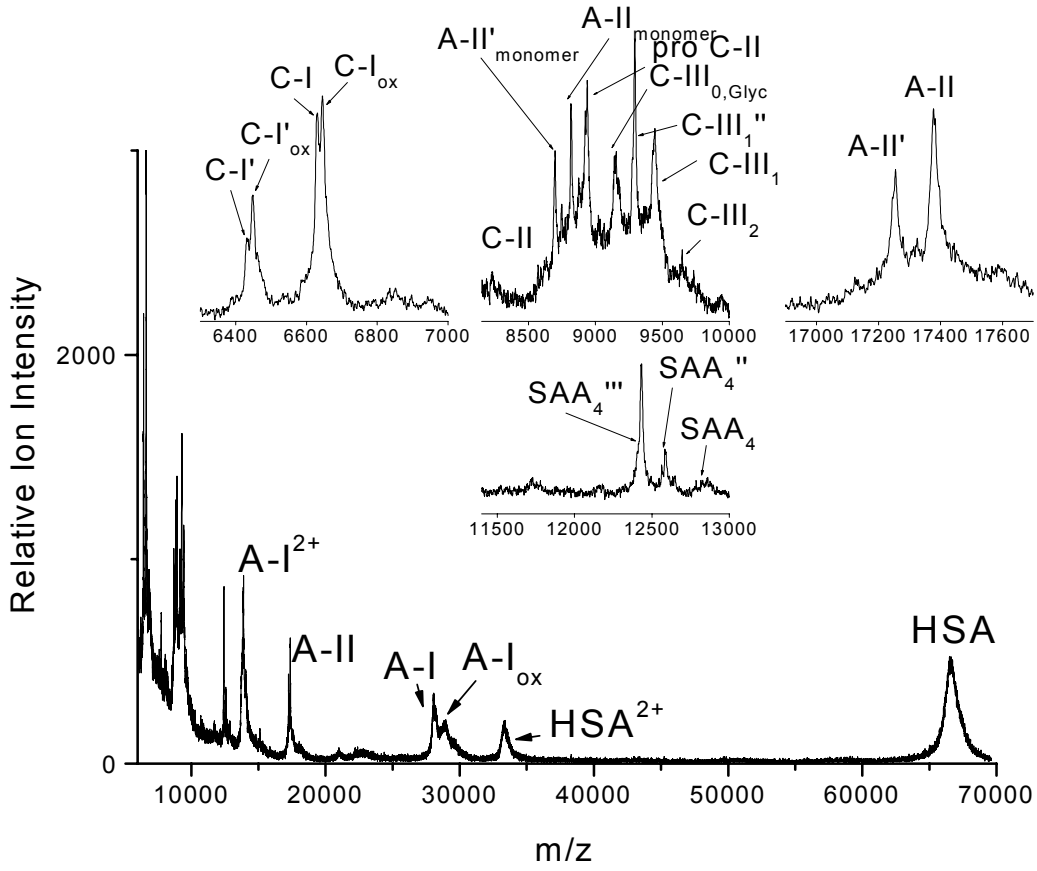

Figure 47. MALDI-TOF analysis of baseline sample.

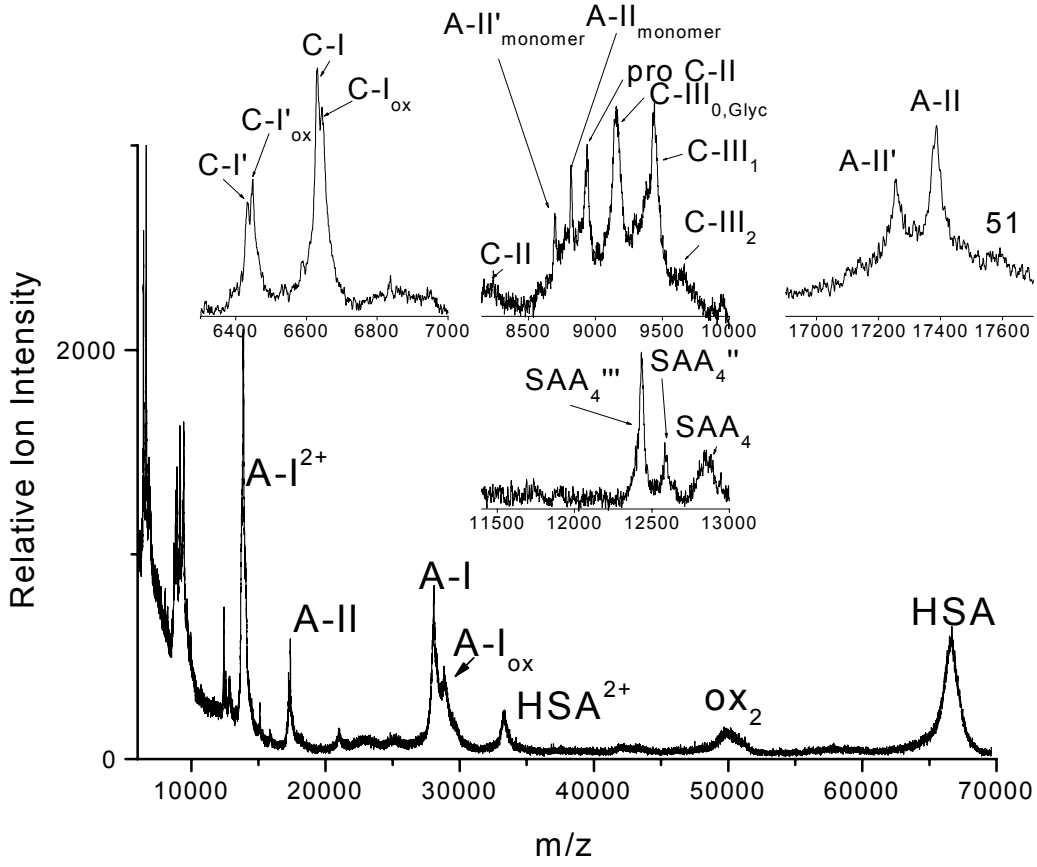

Figure 48. MALDI-TOF analysis of one hour sample.

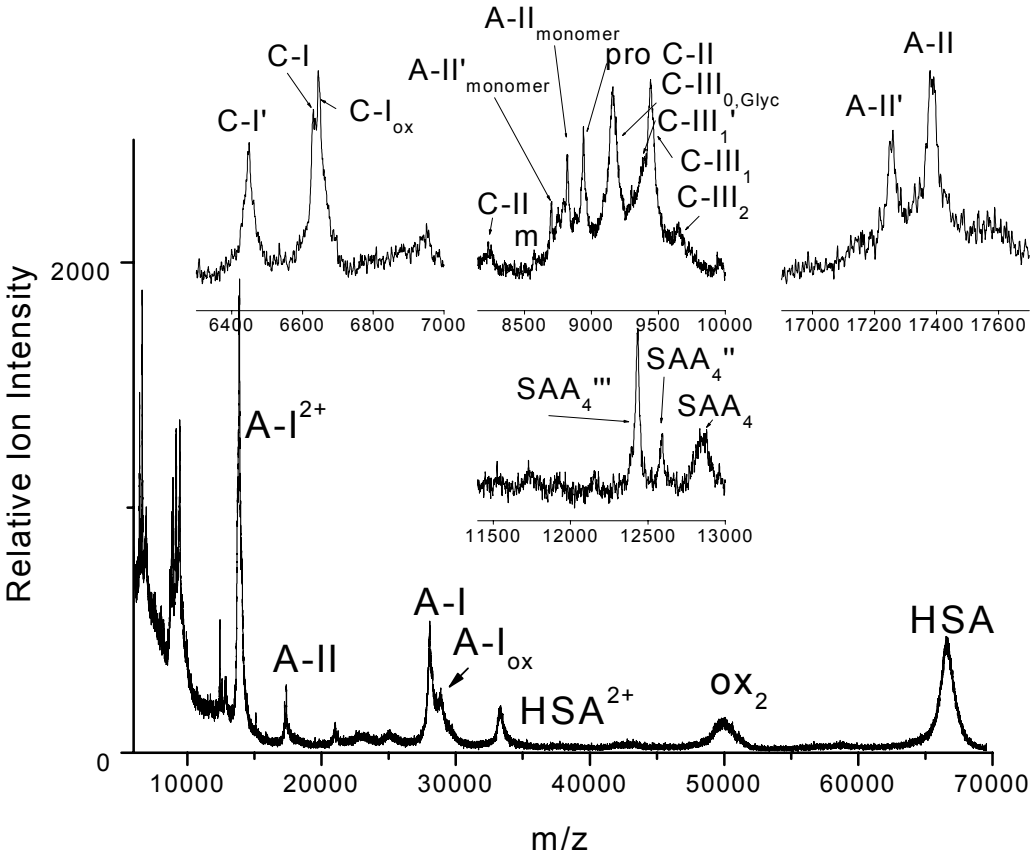

Figure 49. MALDI-TOF analysis of two hour sample.

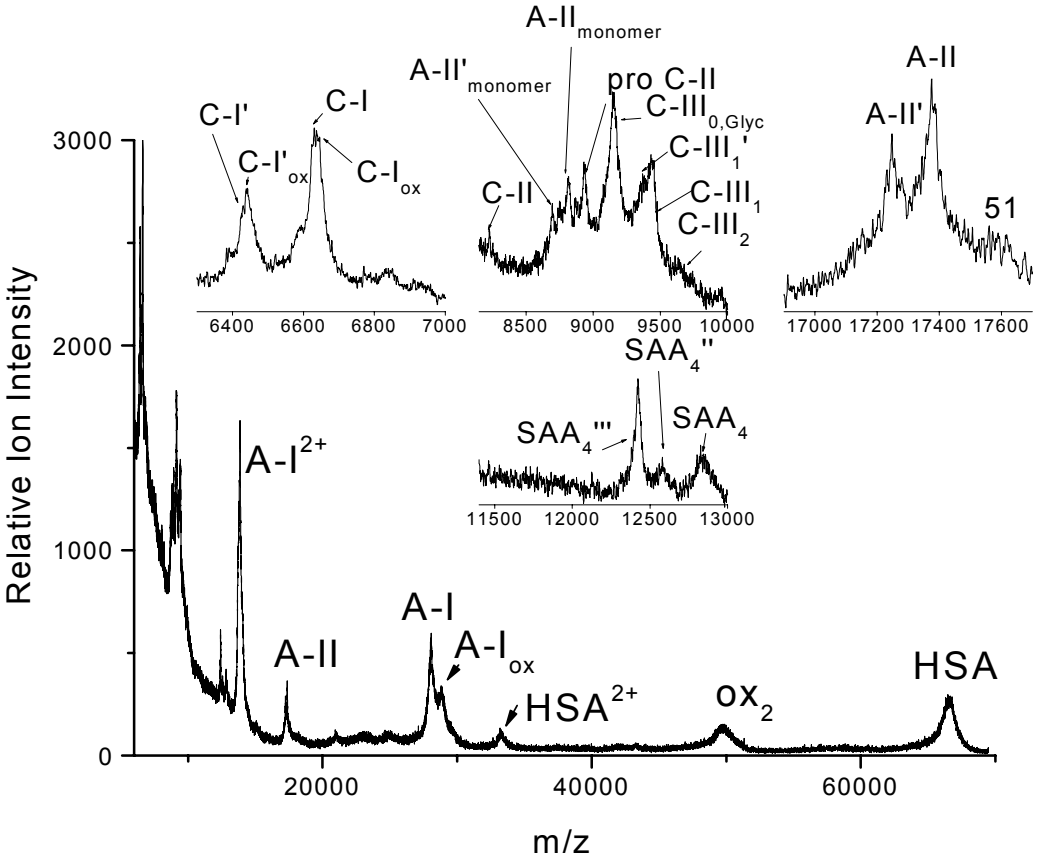

Figure 50. MALDI-TOF analysis of three hour sample.

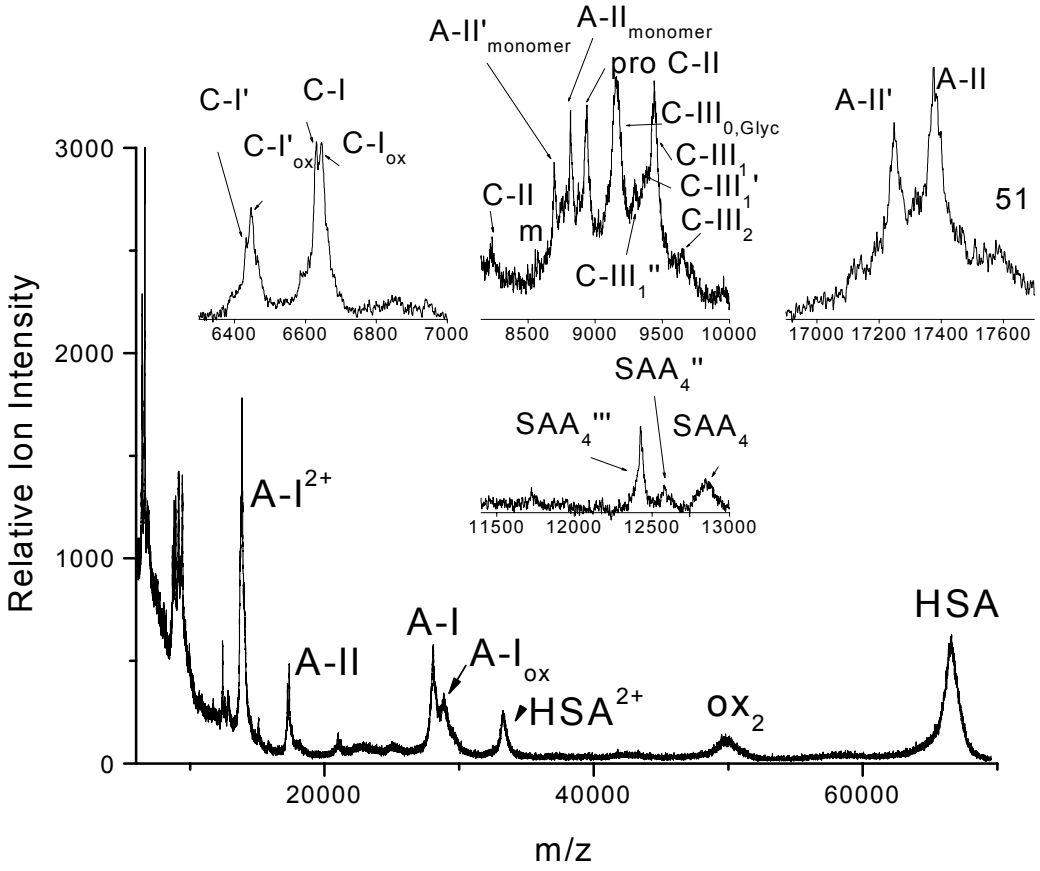

Figure 51. MALDI-TOF analysis of four hour sample.

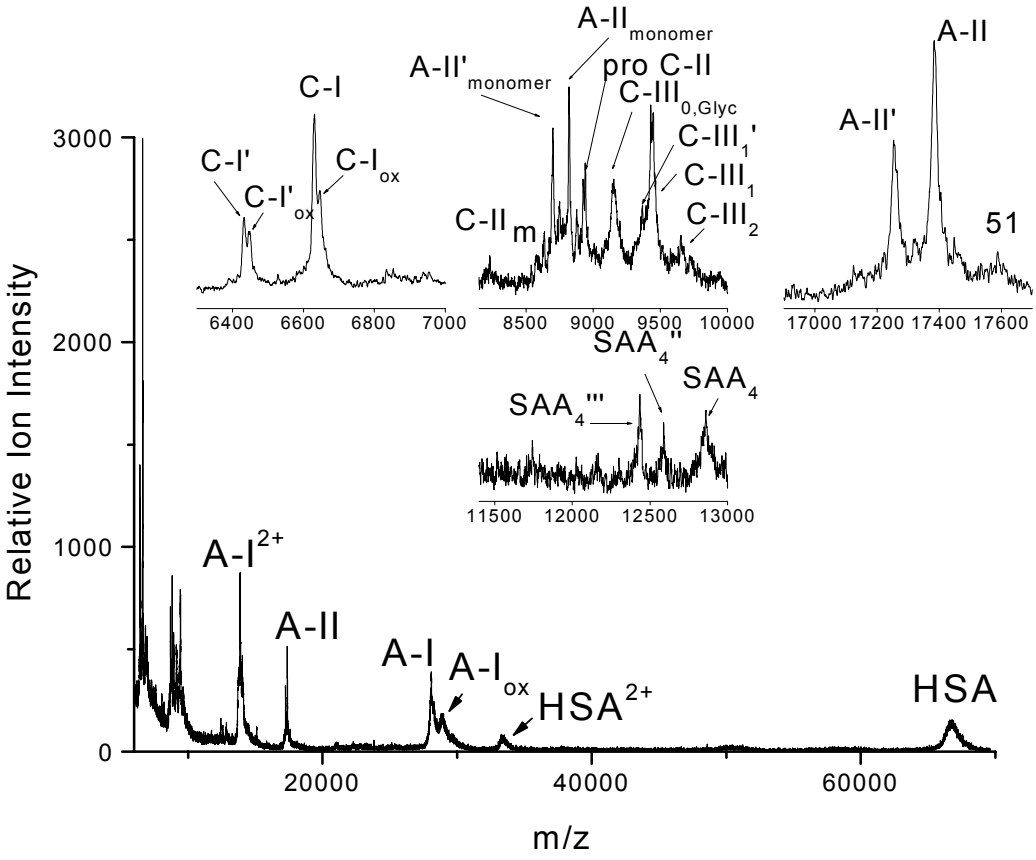

Figure 52. MALDI-TOF analysis of five hour sample.

As expected, dietary grape intake affected the density profile. All oxidized samples showed an increase in mean buoyant density of LDL compared to the control. The baseline sample showed the largest increase (Figure 53), which was expected because the sample contained no antioxidants.

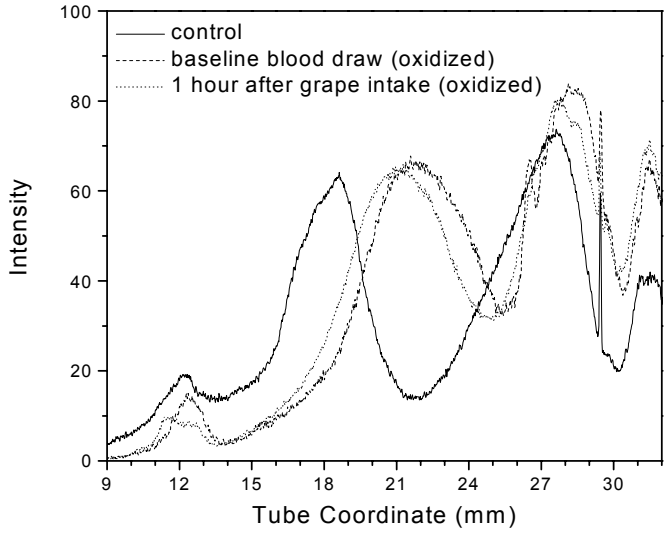

Figure 53. Density profiles as affected by grape consumption.

The one hour serum sample exhibited apparent effects of antioxidants. The LDL density did not shift from the control position as much as in the baseline sample (Figure 53). In the two hour sample, the LDL mean density increased from that observed with the one hour sample. This effect is most likely due to the antioxidants being cleared from the bloodstream over time (127). Three and four hour samples had continuing increasing mean densities but did not reach the level of the baseline sample. The

antioxidants were expected to have continued to clear from the bloodstream leaving only low concentrations.

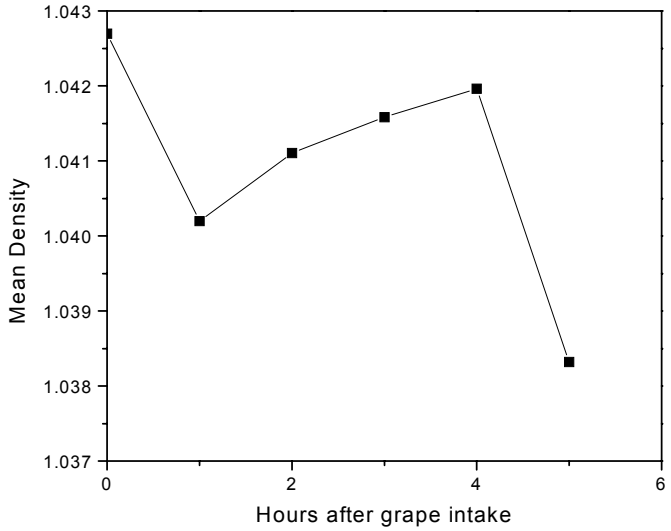

Figure 54. Shift in LDL mean density after grape consumption.

In the five hour sample, the LDL mean density shifted less than any other sample (Figure 54). This observation was unexpected due to the belief that the antioxidants from the grape would clear the bloodstream, and shifts in LDL density would be equal to that seen in the baseline sample. Due to this unexpected density shift in the five hour sample, the oxidation and ultracentrifugation steps were repeated to verify the results. Because it is known that grapes contain multiple types of antioxidant molecules, a hypothesis to explain the small LDL density shift five hours after grape intake would be

that the different antioxidants protect at different time intervals. Initial protection begins immediately, as evidenced by the decreased LDL density shift in the one hour sample. After approximately four hours, a secondary antioxidant mechanism begins protection. This secondary protector is more efficient, as the LDL density shift is smaller than that seen with the one hour sample.

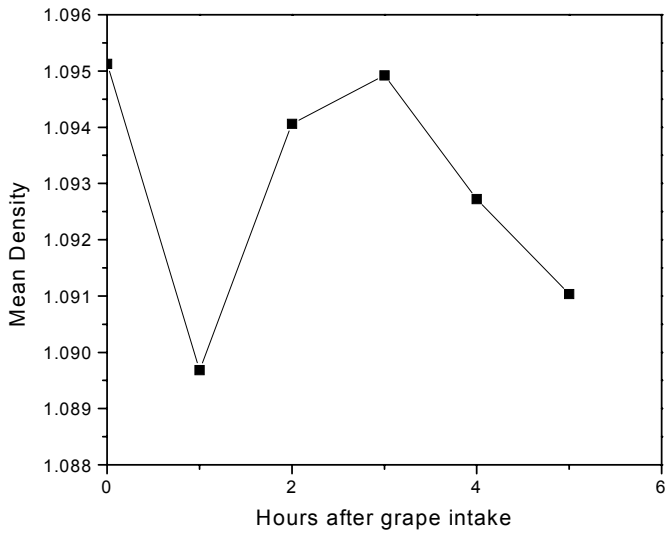

Figure 55. Shift in HDL mean density after grape consumption.

Shifts in HDL mean buoyant density showed similar trends (Figure 55). The baseline sample exhibited a large shift in density, and the one hour sample a smaller shift. The two and three hour samples showed increasingly larger density shifts. However, smaller density shifts were observed in the four and five hour samples, similar

to the five hour LDL sample. The same hypothesis can be used to explain this phenomenon in the HDL as in the LDL.

As was noted in previous AAPH oxidation studies, the shapes of the LDL and HDL density peaks do not change following oxidation. This similarity suggests that the antioxidants from the grape powder protect the entire population of lipoprotein particles.

MALDI-TOF-MS analysis of the oxidized and unoxidized samples reaffirmed the conclusion that MS is a useful tool in oxidized lipoprotein analysis. In addition to the changes noted in the method development section, a new peak was observed at approximately 50000 Da in four of the oxidized samples (labeled ox_2). It is unclear what oxidative process forms this species.

In order to determine if the changes in the mass spectra were proportional to hypothesized level of oxidation, peak area ratios were examined. The area of peaks in the mass spectra are automatically calculated in the software on the mass spectrometer. Peak area ratios of major proteins that show oxidative modifications were calculated and are shown in Table 6.

Table 6. Summary of peak ratios.

Ratio	Control	Baseline	1 hour	2 hour	3 hour	4 hour	5 hour
C-I'/C-I'$_{ox}$	-	0.337	0.429	-	.526	0.680	1.037
C-I/C-I$_{ox}$	-	0.689	0.928	0.398	18.549	0.363	1.387
SAA_4'''/SAA_4''	0.468	7.356	9.756	2.523	22.123	9.904	2.418
SAA_4'''/SAA_4	0.027	53.613	5.588	9.644	9.520	24.242	2.221
SAA_4''/SAA_4	0.057	7.2884	0.573	3.822	0.430	2.448	0.919
A-I/new peak	-	0.467	10.555	5.467	1.578	2.650	6.014

None of the calculated ratios demonstrated a proportionality to the hypothesized level of oxidation of the sample. Further studies need to be done with more samples to determine if any peak area ratio is significantly changed over the oxidative process.

SUMMARY AND CONCLUSIONS

The main objective of this research was to develop a protocol for *in vitro* oxidation of human lipoproteins, and to monitor the oxidation with novel detection methods. Density gradient ultracentrifugation and MALDI-TOF-MS were the analytical techniques chosen for the oxidation studies.

Oxidation of human serum was performed using AAPH, a free radical initiator. A volume studying indicated that oxidation efficiency was higher in smaller volumes of sample. For 100 μL of sample, a time study was run to determine that six hours was a satisfactory incubation time for measurable oxidation.

All oxidation studies were monitored using the TBARS assay. In order to accommodate small sample volumes, a new procedure was developed that required only 50 μL of sample. Using this new protocol, it was determined that increasing incubation time does in fact increase the TBARS response. The maximum of the TBARS chromophore is cited to lie at 532 nm; however my experimental data shows it at 540 nm. Data taken at each wavelength were comparable, and measurements were continued at 532 nm to comply with convention. The TBARS assay is a satisfactory method for fast determination of extent of oxidation in clinical samples, however its lack of specificity requires another detection method to be used simultaneously.

Density gradient ultracentrifugation was used to determine the change in mean buoyant density of the lipoproteins following oxidation. The shift in LDL density (as measured by tube coordinate) over time is very similar to the TBARS response at 532

nm, indicating the density shift is indeed due to oxidation. HDL also shows mean density shifts, although they are not as significant as those seen in LDL. Determination of shift in mean buoyant density of lipoprotein classes is also clinically feasible, and an excellent addition to the TBARS assay.

Two fluorescent probes were examined for their use in density profiling. The first, NBD, was very successful in both CsBiY and NaBiY density gradients for profiling both unoxidized and oxidized samples. The second, NR, did not show the same density shift between unoxidized and oxidized lipoprotein samples. NR has lower fluorescence intensity than NBD in CsBiY, and an even lower intensity in NaBiY. The decrease in intensity causes much detail to be eliminated from the density profile.

Two types of sample, human serum and human plasma, were studied. Density profiles showed few differences between the two. Two types of unoxidized controls were examined; one that was kept frozen at -85°C until analysis, and one that was incubated at 37°C. TBARS analysis showed little difference for the two, indicating no oxidation took place in either sample due to incubation alone. For oxidation times of 24 hours, however, there were distinct differences in the density profiles. When the oxidation time was decreased to 15 hours, the density profiles showed no mean density shifts in the lipoproteins.

The fluorescent probes utilized in the density profiling were also studied for their ability to distinguish small changes in their microenvironment. NBD showed no change between oxidized and unoxidized samples. The NR, however, showed an increase in both emission and excitation maxima for oxidized samples. Further analysis of the

fluorescence maxima shift gave inconsistent results, and the decision was made to forego further study of this phenomena.

MALDI-TOF-MS was used to study oxidative differences in the apoproteins from the HDL fraction. Apo C-I and apo C-I' each split into a doublet, with a m/z difference of 16 Da indicating conversion of a methionine residue to a sulfoxide. The isoform distribution of SAA_4 reversed, indicating oxidation may contribute to truncation. SAA_4'' showed an increased m/z of 16 Da, which could also be due to methionine conversion. Apo A-I also formed a doublet, differing in approximately 800 Da, though more work must be done to distinguish the mechanism of this change. Several other apoproteins exhibited altered m/z ratios of unknown origin. Apo C-II and apo A-$II_{monomer}$ increased by 10 Da, and apo C-$III_{0, Gly}$ increased by 11 Da. A new peak was observed at 13870 m/z, the origin of which is also unknown.

While much work still needs to be done on these methods, they demonstrate without doubt that they are capable of distinguishing between unoxidized and oxidized samples. To further support this claim, a pilot clinical study was conducted to examine the antioxidant effect of California table grapes. Density profiles showed significant shifts in LDL and HDL mean buoyant density. MALDI-TOF-MS illustrated differences as well, however no peak ratio demonstrated a proportionality to the hypothesized oxidation level.

REFERENCES

1. Heart disease and stroke statistics-2004 update. American Heart Association. http://www.americanheart.org/downloadable/heart/1075102824882HDSStats2004UpdateREV1-23-04.pdf.

2. Itabe, H. 2003. Oxidized low-density lipoproteins: What is understood and what remains to be clarified. *Biol. Pharm. Bull.* **1**:1-9.

3. Brown, M.S. and J.L. Goldstein. 1983. Lipoprotein metabolism in the macrophage: Implications for cholesterol deposition in atherosclerosis. *Ann. Rev. Biochem.* **52**:223-261.

4. Scanu, A.M. and Spector, A.A. Biochemistry and Biology of Plasma Lipoproteins. 2nd edition. 1986. Marcel Dekker, Inc., New York, NY.

5. Esterbauer, H., G. Jurgens, O. Quehenberger and E. Koller. 1987. Autoxidation of human low density lipoprotein: Loss of polyunsaturated fatty acids and vitamin E and generation of aldehydes. *J. Lipid Res.* **28**:495-509.

6. Esterbauer, H., J. Gebicki, H. Puhl, and G. Jurgens. 1992. The role of lipid peroxidation and antioxidants in oxidative modification of LDL. *Free Rad. Bio. Med.* **13**:341-390.

7. Loughrey, C. and I. Young. 2000. Indirect assays of lipid peroxidation. *In* Handbook of Lipoprotein Testing. 2nd Edition. N. Rifai, G.R. Warnick, and M. H. Dominiczak, editors. AACC Press, Washington DC. 441-464.

8. Chait, A., R.L. Brazg, D.L. Tribble, and R.M. Krauss. 1993. Susceptibility of small, dense, low-density lipoproteins to oxidative modification in subjects with the atherogenic lipoprotein phenotype, pattern B. *Am. J. Med.* **94**:350-356.

9. Tribble, D.L., M. Rizzo, A. Chait, D.M. Lewis, P.J. Blanche, and R.M. Krauss. 2001. Enhanced oxidative susceptibility and reduced antioxidant content of metabolic precursors of small, dense low-density lipoproteins. *Am. J. Med.* **110**:103-110.

10. Walzem, R.L., S. Watkins, E.N. Frankel, R.J. Hansen, and J.B. German. 1995. Older plasma lipoproteins are more susceptible to oxidation: A linking mechanism for the lipid and oxidation theories of atherosclerotic cardiovascular disease. *Proc. Natl. Acad. Sci. USA*. **92**:7460-7464.

11. Lawn, R.M. 1992. Lipoprotein (a) in heart disease. *Sci. Am.* **266**:54-60.

12. Sobal, G., J. Menzel and H. Sinzinger. 2000. Why is glycated LDL more sensitive to oxidation than native LDL? A comparative study. *Prostaglandins Leuko. Essent. Fatty Acids.* **63**:177-186.

13. Goldstein, J.L., M.S. Brown. 1977. The low-density lipoprotein pathway and its relation to atherosclerosis. *Ann. Rev. Biochem.* **46**:897-930.

14. Mahley, R.W., T.L. Innerarity, K.H. Weisgraber, and S.Y. Oh. 1979. Altered metabolism (*in vivo* and *in vitro*) of plasma lipoproteins after selective chemical modification of lysine residues of the apoproteins. *J. Clin. Invest.* **64**:743-750.

15. Goldstein, J.L., Y.K.Ho, S.K. Basu, and M.S. Brown. 1979. Binding site on macrophages that mediates uptake and degradation of aetylated low density lipoprotein, producing massive cholesterol deposition. *Proc. Natl. Acad. Sci. USA*. **76**:333-337.

16. Fogelman, A.M., I. Shechter, J. Seager, M. Hokom, J.S. Child, and P.A. Edwards. 1980. Malondialdehyde alteration of low density lipoproteins leads to cholesteryl ester accumulation in human monocyte-macrophages. *Proc. Natl. Acad. Sci. USA.* **77**:2214-2218.

17. Henriksen, T., E.M. Mahoney, and D. Steinberg. 1981. Enhanced macrophage degradation of low density lipoprotein previously incubated with cultured endothelial cells: Recognition by receptors for acetylated low density lipoproteins. *Proc. Natl. Acad. Sci. USA.* **78**:6499-6503.

18. Hessler, J.R., D.W. Morel, L.J. Lewis, and G.M.Chisolm. 1983. Lipoprotein oxidation and lipoprotein-induced cytotoxicity. *Arteriosclerosis.* **3**:215-222.

19. Morel, D.W., J.R. Hessler, and G.M. Chisolm. 1983. Low density lipoprotein cytotoxicity induced by free radical peroxidation of lipid. *J. Lipid Res.* **24**:1070-1076.

20. Iuliano, L., F. Micheletta, and F. Violi. 2001. Low-density lipoprotein oxidation. *Ital. Heart J.* **2**:867-872.

21. Salonen, J.T., S. Yla-Herttuala, R. Yamamoto, S. Butler, H. Korpela, R. Salonen, K. Nyyssonen, W. Palinski, and J.L. Witztum. 1992. Autoantibody against oxidized LDL and progression of carotid atherosclerosis. *Lancet.* **339**:883-887.

22. Hodis, H.N., D.M. Kramsch, P.Avogaro, G. Bittolo-Bon, G. Cazzolato, J. Hwang, H. Peterson, and A. Sevanian. 1994. Biochemical and cytotoxic characteristics of an *in vivo* circulating oxidized low density lipoprotein. *J. Lipid Res.* **35**:669-677.

23. Parthasarathy, S., U.P. Steinbrecher, J. Barnett, J.L. Witztum, and D. Steinberg. 1985. Essential role of phospholipase A2 activity in endothelial cell-induced modification of low density lipoprotein. *Proc. Natl. Acad. Sci. USA.* **82**:3000-3004.

24. Devaraj, S. and I. Jialal. 2000. Direct measures of lipid peroxidation. *In* Handbook of Lipoprotein Testing. 2nd Edition. N. Rifai, G.R. Warnick, and M. H. Dominiczak, editors. AACC Press, Washington DC. 441-464.

25. Burton, G.W. and K.U. Ingold. 1984. An unusual type of lipid antioxidant. *Science.* **224**:569-573.

26. Stocker, R., V.W. Bowry, and B. Frei. 1991. Ubiquinol-10 protects human low-density lipoprotein more efficiently against lipid peroxidation than does alpha-tocopherol. *Proc. Natl. Acad. Sci. USA.* **88**:1646-1650.

27. Kontush, A., S. Chantepie, and M.J. Chapman. 2003. Small, dense HDL particles exert potent protection of atherogenic LDL against oxidative stress. *Arterioscler. Thromb. Vasc. Biol.* **23**:1881-1888.

28. Sarandol, E., Z. Serdar, M. Dirican, O. Safak. 2003. Effects of red wine consumption on serum paraoxonase/arylesterase activities and on lipoprotein oxidizability in healthy-men. *J. Nutr. Biochem.* **14**:507-512.

29. Navab, M., S.Y. Hama, G.M. Anantharamaiah, K. Hassan, G.P. Hough, A.D. Watson, S.T. Reddy, A. Sevanian, G.C. Fonarow, and A.M. Fogelman. 2000. Normal high density lipoprotein inhibits three steps in the formation of mildly oxidized low density lipoprotein: steps 2 and 3. *J. Lipid Res.* **41**:1495-1508.

30. Podrez, E.A., D. Schmitt, H.F. Hoff, and S.L. Hazen. 1999. Myeloperoxidase-generated reactive nitrogen species convert LDL into an atherogenic form *in vitro*. *J. Clin. Invest.* **103**:1547-1560.

31. Tsimikas, S. and J.L. Witztum. 2001. Measuring circulating oxidized low-density liporotein to evaluate coronary risk. *Circulation.* **103**:1930-1932.

32. Witztum, J.L. and D. Steinberg. 1991. Role of oxidized low density lipoprotein in atherogenesis. *J. Clin. Invest.* **88**:1785-1792.

33. Shaikh, M., R. Wootton, B.G. Nordestgaard, P. Baskerville, J.S. Lumley, A.E. La Ville, J. Quiney, and B. Lewis. 1991. Quantitative studies of transfer *in vivo* of low density, sf12-60, and sf 60-400 lipoproteins between plasma and arterial intima in humans. *Arterioscler. and Thromb.* **11**:569-577.

34. Avogaro, P., G.B. Bon, and G. Cazzolato. 1988. Presence of a modified low density lipoprotein in humans. *Arteriosclerosis.* **8**:79-87.

35. Sevanian, A., J. Hwang, H. Hodis, G. Cazzolato, P. Avogaro, and G. Bittolo-Bon. 1996. Contribution of an *in vivo* oxidized LDL to LDL oxidation and its association with dense LDL subpopulations. *Arterioscler. Thromb. Vasc. Biol.* **16**:784-793.

36. Jialal, I. and S. Devaraj. 1996. Low-density lipoprotein oxidation, antioxidants, and atherosclerosis: A clinical biochemistry perspective. *Clin. Chem.* **42**:498-506.

37. Steinbrecher, U.P., J.L. Witztum, S. Parthasarathy, and D. Steinberg. 1987. Decrease in reactive amino groups during oxidation or endothelial cell modification of LDL. *Arteriosclerosis.* **7**:135-143.

38. Jialal, I. and A. Chait. 1989. Differences in the metabolism of oxidatively modified low density lipoprotein and acetylated low density lipoprotein by human endothelial cells: Inhibition of cholesterol esterification by oxidatively modified low density lipoprotein. *J. Lipid Res.* **30**:1561-1568.

39. Panasenko, O.M., T.V. Vol'nova, O.A. Azizova, and Y.A. Vladimirov. 1991. Free radical modification of lipoproteins and cholesterol accumulation in cells upon atherosclerosis. *Free Rad. Bio. Med.* **10**:137-148.

40. Henriksen, T., E.M. Mahoney, and D. Steinberg. 1983. Interactions of plasma lipoproteins with endothelial cells. *Ann. N.Y. Acad. Sci.* **401**:102-116.

41. Henriksen, T., E.M. Mahoney, D. Steinberg. 1983. Enhanced macrophage degradation of biologically modified low density lipoprotein. *Arteriosclerosis.* **3**:149-159.

42. Steinberg, D. 1988. Metabolism of lipoproteins and their role in the pathogenesis of atherosclerosis. *Atheroscler. Rev.* **18**:1-23.

43. Jurgens, G., J. Lang, and H. Esterbauer. 1986. Modification of human low-density lipoprotein by the lipid peroxidation product 4-hydroxynonenal. *Biochim. Biophys. Acta.* **875**:103-114.

44. Berlett, B.S., and E.R. Stadtman. 1997. Protein oxidation in aging, disease, and oxidative stress. *J. Biol. Chem.* **272**:20313-20316.

45. Fong, L.G., S. Parthasarathy, J.L. Witztum, and D. Steinberg. 1987. Nonenzymatic oxidative cleavage of peptide bonds in apoprotein B-100. *J. Lipid Res.* **28**:1466-1477.

46. Roubal, W.T. and A.L. Tappel. 1966. Damage to proteins, enzymes, and amino acids by peroxidizing lipids. *Arch. Biochem. Biophys.* **113**:5-8.

47. Tomita, M., M. Irie, and T. Ukita. 1969. Sensitized photooxidation of histidine and its derivatives producs and mechanism of the reaction. *Biochemistry.* **8**:5149-5160.

48. Steinbrecher, U.P. 1987. Oxidation of human low density liporotein results in derivatization of lysine residues of apoprotein B by lipid peroxide decomposition products. *J. Biol. Chem.* **262**:3603-3608.

49. Parthasarathy, S., D.J. Printz, D. Boyd, L. Joy, and D. Steinberg. 1986. Macrophage oxidadtion of low density liportoein generates a modified form recognized by the scavenger receptor. *Arteriosclerosis.* **6**:505-510.

50. Herpfer, I., J. Greilberger, G. Ledinski, B. Widner, D. Fuchs, and G. Jurgens. 2002. Neopterin and 7,8-dihydroneopterin interere with low density liporotein oxidation mediated by peroxynitrite and or copper. *Free Radic. Res.* **36**:509-520.

51. Hoff, H.F., T.E. Whitaker, and J. O'Neil. 1992. Oxidation of low density lipoprotein leads to particle aggregation and altered macrophage recognition. *J. Biol. Chem.* **267**:602-609.

52. Cominacini, L., U. Garbin, A. Davoli, R. Micciolo, O. Bosello, G. Gaviraghi, L.A. Scuro, and A.M. Pastorino. 1991. A simple test for predisposition to LDL oxidation based on the fluorescence development during copper-catalyzed oxidative modification. *J. Lipid Res.* **32**:349-358.

53. Frei, B., R. Stocker, and B.N. Ames. 1988. Antioxidant defenses and lipid peroxidation in human blood plasma. *Proc. Natl. Acad. Sci. USA.* **85**:9748-9752.

54. Lotito, S.B. and C.G. Fraga. 2000. Catechins delay lipid oxidation and α-tocopherol and β-carotene depletion following ascorbate depletion in human plasma. *Proc. Soc. Exp. Biol. Med.* **225**:32-38.

55. Niki, E. 1990. Free radical initiators as source of water- or lipid-soluble peroxyl radicals. *Methods Enzymol.* **186**:100-108.

56. Tsai, K., T.G. Hsu, C.W. Kong, K.C. Lin, and F.J. Lu. 2000. Is the endogenous peroxyl-radical scavenging capacity of plasma protective in systemic inflammatory disorders in humans? *Free Rad. Bio. Med.* **28**:926-933.

57. Yoshida, Y., N. Ito, S. Shimakawa, and E. Niki. 2003. Susceptibility of plasma lipids to peroxidation. *Biochem. Biophys. Res. Commun.* **305**:747-753.

58. Kohn, H.I. and M. Liversedge. 1944. On a new aerobic metabolite whose production by brain is inhibited by apomorphine, emetine, ergotamine, epinephrine, and menadione. *J. Pharmacol. Exp. Ther.* **83**:292-300.

59. Sinnhuber, R. O., T.C. Yu, and T.C. Yu. 1958. Characterization of the red pigment formed in the 2-thiobarbituric acid determination of oxidative rancidity. *Food Res.* **23**:626-633.

60. Janero, D.R. 1990. Malondialdehyde and thiobarbituric acid-reactivity as diagnostic indices of lipid peroxidation and peroxidative tissue injury. *Free Rad. Bio. Med.* **9**:515-540.

61. Sinnhuber, R.O. and T.C. Yu. 1958. 2-Thiobarbituric acid method for measurement of rancidity in fishery products II. The quantitative determination of malonaldehyde. *Food Tech.* **12**:9-12.

62. Hostmark, A.T. and E. Lystad. 1992. Growth inhibition of human hepatoma cells (HepG2) by polyunsaturated fatty acids. Protection by albumin and vitamin E. *Acta Physiol. Scand.* **144**:83-88.

63. Johansen, O., M. Abdelnoor, M. Brekke, I. Seljeflot, A.T. Hostmark, and H. Arnesen. 2001. Predictors of restenosis after coronary angioplasty. A study on demographic and metabolic variables. *Scand. Cardiovasc. J.* **35**:86-91.

64. Kosugi, H., T. Kojima, and K. Kikugawa. 1989. Thiobarbituric acid-reactive substances from peroxidized lipids. *Lipids.* **24**:873-881.

65. Busserolles, J., A. Mazur, E. Gueux, E. Rock, and Y. Rayssiguier. 2002. Metabolic syndrome in the rat: Females are protected against the pro-oxidant effect of a high sucrose diet. *Exp. Biol. Med.* **227**:837-842.

66. Dinis, T.C.P., C.L. Santos, and L.M. Almeida. 2002. The apoprotein is the preferential target for peroxynitrite-induced LDL damage protection by dietary phenolic acids. *Free Radic. Res.* **36**:531-543.

67. Nourooz-Zadeh, J., J. Tajaddini-Sarmadi, and S.P. Wolff. 1994. Measurement of plasma hydroperoxide concentrations by the ferrous oxidation-xylenol orange assay in conjunction with triphenylphosphine. *Anal. Biochem.* **220**:403-409.

68. Birnie, G.D. 1980. Isopycnic centrifugation in ionic media. *Biochem. Soc. Trans.* **8**:513-515.

69. Hosken, B. 2002. Density gradient ultracentrifugation of lipoproteins using metal ion complex solutes. Ph.D. Dissertation, Texas A&M University, College Station, TX.

70. Belcher, J.D., J.O. Egan, G. Bridgman, R. Baker, and J.M. Flack. 1991. A micro-enzymatic method to measure cholesterol and triglyceride in lipoprotein subfractions separated by density gradient ultracentrifugation from 200 microliters of plasma or serum. *J. Lipid Res.* **32**:359-370.

71. Graham, J.M., J.A. Higgins, T. Gillott, T. Taylor, J. Wilkinson, T. Ford, and D. Billington. 1996. A novel method for the rapid separation of plasma lipoproteins using self-generating gradients of iodixanol. *Atherosclerosis.* **124**:125-135.

72. Foreman, J.R., J.B. Karlin, C. Edelstein, D.J. Juhn, A.H. Rubenstein, and A.M. Scanu. 1977. Fractionation of human serum lipoproteins by single-spin gradient ultracentrifugation: Quantification of apolipoproteins B and A-I and lipid components. *J. Lipid Res.* **18**:759-767.

73. Randolph, M.L. and R.R.Ryan. 1950. A slicer for sampling liquids. *Science.* **112**:528.

74. Swinkels, D.W., H.L.M. Hak-Lemmers, P.N.M. Demacker. 1987. Single spin density gradient ultracentrifugation method for the detection and isolation ofl ight and heavy low density liporotein subfractions. *J. Lipid Res.* **28**:1233-1239.

75. Schjeide, O.A., A.U. Rivin, and J.Yoshino. 1963. Uptake of lipid stains by lipids and serum lipoproteins. *Am. J. Clin. Pathol.* **39**:329-341.

76. Cruzado, I.D., S.L. Cockrill, C.J. McNeal, and R.D. Macfarlane. 1998. Characterization and quantitation of apolipoproteins B-100 by capillary electrophoresis. *J. Lipid Res.* **39**:205-217.

77. Cockrill, S.L. 1998. Lipoprotein density profiling-assessment of cardiovascular risk. Ph.D. Dissertation, Texas A&M University, College Station, TX.

78. Via, D.P. and L.C. Smith. 1986. Fluorescent labeling of lipoproteins. *Methods Enzymol.* **129**:848-857.

79. Chattopadhyay, H. and E. London. 1987. Parallax method for direct measurement of membrane penetration depth utilizing fluorescence quenching by spin-labeled phospholipids. *Biochemistry.* **26**:39-45.

80. Abrams, F.S. and E. London. 1993. Extension of the parallax analysis of membrane penetration depth to the polar region of model membranes: Use of fluorescent quenching by a spin-label attached to the phospholipid polar headgroup. *Biochemistry.* **32**:10826-10831.

81. Chattopadhyay, A. 1990. Chemistry and biology of N-(7-nitrobenz-2-oxa-1,3-diazol-4-yl)-labeled lipids: fluorescent probes of biological and model membranes. *Chem. Phys. Lipids.* **53**:1-15.

82. Weiller, B.H., L. Ceriotti, T. Shibata, D. Rein, M.A. Roberts, J. Lichtenberg, J.B. German, N.F. De Rooij, and E. Verpoorte. 2002. Analysis of lipoproteins by capillary zone electrophoresis in microfluidic devices: Assay development and surface roughness measurements. *Anal. Chem.* **74**:1702-1711.

83. Absorption and emission spectra. Molecular Probes. 2004. http://www.probes.com/servlets/spectra?fileid=316meoh.

84. Greenspan, P., E.P. Mayer, and S.D. Fowler. 1985. Nile red: A selective fluorescent stain for intracellular lipid droplets. *J. Cell Biol.* **100**:965-973.

85. Absorption and emission spectra. Molecular probes. 2004. http://www.probes.com/servlets/spectra?fileid=1142lip.

86. Davis, M.M. and H.B. Hetzer. 1966. Titrimetric and equilibrium studies using indicators related to Nile blue a. *Anal. Chem.* **38**:451-461.

87. Greenspan, P. and S.D. Fowler. 1985. Spectrofluorometric studies of the lipid probe, nile red. *J. Lipid Res.* **26**:781-789.

88. Greenspan, P. and P. Lou. 1993. Spectrofluorometric studies of nile red treated with native and oxidized low density lipoprotein. *Int. J. Biochem.* **25**:987-991.

89. Karas, M. and F. Hillenkamp. 1988. Laser desorption ionization of proteins with molecular masses exceeding 10 000 daltons. *Anal. Chem.* **60**:2299-2301.

90. Karas, M., D. Buchmann, U. Bahr, and F. Hillenkamp. 1987. Matrix-assisted ultraviolet laser desorption of non-volatile compounds. *Int. J. Mass Spectrom. Ion. Processes.* **78**:53-68.

91. Hillenkamp, F., M. Karas, R.C. Beavis, and B.T. Chait. 1991. Matrix-assisted laser desorption/ionization mass spectrometry of biopolymers. *Anal. Chem.* **63**:1193A-1203A.

92. Karas, M., M. Gluckmann, and J. Schafer. 2000. Ionization in matrix-assisted laser desorption/ionization: singly charged molecular ions are the lucky survivors. *J. Mass. Spectrom.* **35**:1-12.

93. Zenobi, R. and R. Knochenmuss. 1998. Ion formation in MALDI mass spectrometry. *Mass Spectrom. Rev.* **17**:337-366.

94. Karas, M. and U. Bahr. 1997. Matrix-assisted laser desorption-ionization (MALDI) mass spectrometry: Principles and applications. *In* Selected Topics and Mass Spectrometry in the Biomolecular Sciences. R.M. Caprioli, editor. Kluwer Academic Publishers, Dordrecht, The Netherlands. 33-35.

95. Beavis, R.C. and B.T. Chait. 1989. Cinnamic acid derivatives as matrices for ultraviolet laser desorption mass spectrometry of proteins. *Rapid Commun. Mass Spectrom.* **3**:432-435.

96. Beavis, R.C. and J.N. Bridson. 1993. Epitaxial protein inclusion in sinapic acid crystals. *J. Physics D: Appl. Phys.* **26**:442-447.

97. Vorm, O., P. Roepstorff, and M. Mann. 1994. Improved resolution and very high sensitivity in MALDI TOF of matrix made by fast evaporation. *Anal. Chem.* **66**:3281-3287.

98. Bonk, T., and A. Humeny. 2001. MALDI-TOF-MS analysis of protein and DNA. *Neuroscientist.* **7**:6-12.

99. Beavis, R.C. and B.T. Chait. 1990. Rapid, sensitive analysis of protein mixtures by mass spectrometry. *Proc. Natl. Acad. Sci. USA.* **87**:6873-6877.

100. Bondarenko, P.V. 1998. Profiling human plasma apolipoproteins by mass spectrometry. Ph.D. Dissertation. Texas A&M University, College Station, TX.

101. Bondarenko, P.V., Z.N. Farwig, C.J. McNeal, and R.D. Macfarlane. 2002. MALDI- and ESI-MS of the HDL apolipoproteins; new isoforms of apo A-I, A-II. *Int. J. Mass Spectrom. Ion Processes.* **219**:671-680.

102. Farwig, Z.N. 2002. Lipoproteomics: Multi-dimensional analysis of human serum apolipoproteins. Ph.D. Dissertation. Texas A&M University, College Station, TX.

103. Bondarenko, P.V., I.D. Cruzado, S.L. Cockrill, L.K. Watkins, and R.D. Macfarlane. 1999. Mass spectral study of polymorphism of the apolipoproteins of very low density lipoproteins. *J. Lipid Res.* **40**:543-555.

104. von Eckardstein, A., M. Walter, H. Holz, A. Benninghoven, G. Assmann, A. Roetrige, and R. Kock. 1991. Site-specific methionine sulfoxide formation is the structural basis of chromatographic heterogeneity of apolipoproteins A-I, C-II, and C-III. *J. Lipid Res.* **32**:1465-1476.

105. Anantharamaiah, G.M., T.A. Hughes, M. Iqbal, A. Gawish, P.J. Neame, M.F. Medley, and J.P. Segrest. 1988. Effect of oxidation on the properties of apolipoproteins A-I and A-II. *J. Lipid Res.* **29**:309-318.

106. Pankhurst, G., X.L. Wang, D.E. Wilcken, G. Baernthaler, U. Panzenbock, M. Raftery, and R. Stocker. 2003. Characterization of specifically oxidized apolipoproteins in mildly oxidized high density lipoprotein. *J. Lipid Res.* **44**:349-355.

107. Pazenbock, U., L. Kritharides, M. Faftery, K.A. Rye, and R. Stocker. 2000. Oxidation of methionine residues to methionine sulfoxides does not decrease potential antiatherogenic properties of apolipoproteins A-I. *J. Biol. Chem.* **275**:19536-19544.

108. Hosken, B.D. and R.D. Macfarlane. 2002. Density gradient solutions of metal ion complexes. U.S. patent 10/092,032,2002.

109. Watkins, L.K., P.V. Bondarenko, D.C. Barbacci, S. Song, S.L. Cockrill, D.H. Russell, and R.D. Macfarlane. 1999. Fast C_{18} solid-phase desalting/delipidation of the human serum apolipoproteins for matrix-assisted laser desorption ionization and electrospray ionization mass spectrometric analysis. *J. Chromatogr. A.* **840**:183-193.

110. Cobbold, C.A., J.A. Sherratt, and S.R.J. Maxwell. 2002. Lipoprotein oxidation and its significance for atherosclerosis: A mathematical approach. *Bull. Math. Bio.* **64**:65-95.

111. Soutar, A.K., C.W. Garner, H.N. Baker, J.T. Sparrow, R.L. Jackson, A.M. Gotto, and L.C. Smith. 1975. Effect of the human plasma apolipoproteins and

phosphatidylcholine acyl donor on the activity of lecithin:cholesterol acyltransferase. *Biochemistry.* **14**:3057-3064.

112. Gabelli, C., C. Bilato, S. Santamarina-Fojo, S. Martini, H.B. Brewer Jr., G. Crepaldi, and G. Baggio. 1993. Heterozygous apolipoproteins C-II deficiency: Lipoprotein and apoprotein phenotype and rsal restriction enzyme polymorphism in the Apo C-II_{padova} kindred. *Eur. J. Clin. Invest.* **23**:522-528.

113. Glomset, J.A. 1968. The plasma lecithin:cholesterol acyltransferase reaction. *J. Lipid Res.* **9**:155-167.

114. Bondarenko, P.V., I.D. Cruzado, S.L. Cockrill, L.K. Watkins, and R.D. Macfarlane. 1999. Mass spectral study of polymorphism of the apolipoproteins of very low density lipoproteins. *J. Lipid Res.* **40**:543-555.

115. Bier, D.M. and R.J. Havel. 1970. Activation of lipoprotein lipase by lipoprotein fractions of human serum. *J. Lipid Res.* **11**:565-570.

116. LaRosa, J.C., R.I. Levy, P. Herbert, S.E. Lux, and D.S. Fredrickson. 1970. A specific apoprotein activator for lipoprotein lipase. *Biochem. Biophys. Res. Commun.* **41**:57-62.

117. Ikeda, Y., A. Takagi, and A. Yamamoto. 1989. Purification and characterization of lipoprotein lipase and hepatic triglyceride lipase from human postheparin plasma: Production of monospecific antiobody to the individual lipase. *Biochim. Biophys. Acta.* **1003**:254-269.

118. Mahley, R.W., T.L. Innerarity, S.C. Rall, Jr., and K.H. Weisgraber. 1984. Plasma lipoproteins: Apolipoproteins structure and function. *J.Lipid Res.* **25**:1277-1292.

119. Strachan, A.F., E.G. Shephard, D.U. Bellstedt, G.A. Coetzee, D.R. Van der Westhuyzen, and F.C. DeBeer. 1989. Human serum amyloid A protein. *Biochem. J.* **263**:365-370.

120. Strachan, A.F., W.F. Brandt, P. Woo, D.R. Van der Westhuyzen, G.A. Coetzee, M.C. DeBeer, E.G. Shephard, and F.C. DeBeer. 1989. Human serum amyloid A protein. *J. Biol. Chem.* **264**:18368-18373.

121. Whitehead, A.S., M.C. DeBeer, D.M. Steel, M. Rits, J.M. Lelias, W.S. Lane, and F.C. DeBeer. 1992. Identification of novel members of the serum amyloid A protein superfamily as constitutive apolipoproteins of high density lipoprotein. *J. Biol. Chem.* **267**:3862-3867.

122. Blanco-Vaca, F., J. C. Escola-Gil, J.M. Martin-Campos, and J. Julve. 2001. Role of apoA-II in lipid metabolism and atherosclerosis: advances in the study of an enigmatic protein. *J. Lipid Res.* **32**:1727-1739.

123. Hedrick, C.C., L.W. Castellani, H. Wong, and A.J. Lusis. 2001. *In vivo* interactions of apoA-II, apoA-I, and hepatic lipase contributing to HDL structure and antiatherogenic functions. *J. Lipid Res.* **42**:563-570.

124. Renaud, S. and M. de Lorgeril. 1992. Wine, alcohol, platelets, and the French paradox for coronary heart disease. *Lancet.* **339**:1523-1526.

125. Frankel, E.N. and A.S. Meyer. 1998. Antioxidants in grapes and grape juices and their potential health effects. *Pharm. Biol.* **36**:14-20.

126. Meyer, A.S., O.-M. Yi, D.A. Pearson, A.L. Waterhouse, and E.N. Frankel. 1997. Inhibition of human low-density lipoprotein oxidation in relation to composition of phenolic antioxidants in grapes (*Vitis vinifera*). *J. Agric. Food Chem.* **45**:1638-1643.

127. Chow, H.H.S., Y. Cai, D.S. Alberts, I. Hakim, ,R. Dorr, F. Shahi, J.A. Crowell, C.S. Yang, and Y. Hara. 2001. Phase I pharmacokinetic study of tea polyphenols following single-dose administration of epigallocatechin gallate and polyphenon E. *Cancer Epidemiol. Biomarkers Prev.* **10**:53-58.

VITA

Christine Lee Myers graduated from The Colorado College in May of 2000 with a B.A. in biochemistry. In June of that same year, she began her graduate career at Texas A&M University, in the laboratory of Dr. Ronald D. Macfarlane. Christine's research involved the detection of oxidized lipoproteins in human serum. She defended her research in February of 2004, and received her Master of Science in May of 2004. The author may be reached at 836 Elliott Street, Longmont, CO, 80501.